SUM4Re

Creating materials banks
from digital urban mining

# D2.5 GPR-ECT methodological framework acquisition

VERSION 1.0

28 October 2025

PUBLIC

Associated with document Ref. 101129961

Funded by the European Union. Views and opinions expressed are however those of the author(s) only and do not necessarily reflect those of the European Union. Neither the European Union nor the granting authority can be held responsible for them.

Funded by the European Union

SUM4Re

Creating materials banks from digital urban mining

| | |
|---|---|
| **Deliverable ID** | D2.5 |
| **Deliverable name** | GPR-ECT methodological framework acquisition |
| **Lead partner** | EAGLE |
| **Contributors** | MOYUA, NORSKE, SINTEF, AFDECOM |

PUBLIC





Funded by the European Union

# DOCUMENT INFORMATION

| | |
|---|---|
| **Document name** | D2.5 GPR-ECT methodological framework acquisition |
| **Version** | 1.0 |
| **Due date** | 31/10/2025 |
| **Report date** | 28/10/2025 |
| **Number of pages** | 51 |
| **Lead Author** | Ourania Patsia (EAGLE), Alex Novo (EAGLE) |
| **Other Authors** | - |
| **Dissemination level** | Public |

# REVISION HISTORY

| Rev. | Date | Description of revision |
|---|---|---|
| 0.1 | 30/09/2025 | Initial version |
| 0.2 | 23/10/2025 | Revised draft |
| 1.0 | 28/10/2025 | Final version |

# DOCUMENT APPROVAL

| | | |
|---|---|---|
| **Written** | Alex Novo (EAGLE), Ourania Patsia (EAGLE) | 30/09/2025 |
| **Revised** | Jose Carlos Jimenez (TECN), Francisco Senna Vieira (VTT) | 15/10/2025 |
| | Ana Sánchez (UVIGO, Project Manager) | 28/10/2025 |
| **Approved** | Pedro Arias Sánchez (UVIGO, Project Coordinator) | 28/10/2025 |

# EXECUTIVE SUMMARY

Deliverable D2.5 for Task 2.5 provides a methodological framework for applying Ground Penetrating Radar (GPR) and Eddy Current Technology (ECT) for identifying construction materials from end-of-life buildings that can be reused to new constructions or for renovation purposes, as part of Work Package 2 (WP2). Both technologies provide complimentary capabilities for detecting and locating hidden structural elements and assessing material conditions in buildings, making them valuable tools for selective deconstruction in the construction sector.

This document presents information on the state of the art for both technologies, their limitations and the materials and information targeted to be found with these technologies as part of the SUM4Re project. The methodology followed includes description and technical specifications of the equipment used, information on the survey setup, data collection, post-processing and interpretation along with hardware and software usage descriptions. Two systems were used for this study, the Proceq GP8800 GPR probe, a handheld step-frequency continuous-wave (SFCW) system and the Proceq PM8000 ECT sensor, a portable handheld sensor designed for rebar detection, diameter and cover depth estimation.

This framework is demonstrated with two case studies. The Spanish pilot, carried out in Jolastokieta in San Sebastian, Spain, focusing on a reinforced concrete structure. Both GPR and ECT were used to identify reinforcing components and assess the condition of concrete. The Nordic pilot, in contrast, focused in examining a timber residential building in Longyearbyen, Svalbard, Norway, where GPR was employed to locate hidden components, such as studs, insulation and others and assess the condition of the structure. This case was particularly relevant for understanding material reuse potential under extreme Arctic conditions.

Initially, prior to the field visit for data collection, certain preparatory measures were taken to support the fieldwork, such as studying available information on the case studies, selecting the appropriate equipment, the scanning locations and samples, coordinating with each case study relevant partners but also certain control measures for mitigating the risks. In addition, in the case of the Nordic pilot, simulations and scanning of a mock-up sample of the external apartment wall were also performed as additional preparation and for acquiring better understanding of the GPR propagation in this type of structures.

During field data collection, several samples were collected from different locations at both case studies. Dense data acquisition was performed to capture as much information as possible from each scanning area. Valuable information could be extracted for both case studies such as assessing the material condition, find weaker areas and potential voids and also identifying hidden objects and layers such as the reinforcement mesh in the Spanish pilot and wooden studs, insulation layers and other components in the case of the Nordic pilot. The successful application of the GPR technology demonstrates its adaptability across diverse construction types.

Despite acquiring successfully significant information regarding the internal structure of the buildings, there are still certain technological and methodological challenges. One limitation was that the ECT sensor could not be used for rebar diameter estimation in the case of the Spanish pilot, as the rebars were deeper than the maximum depth required for diameter estimation. In addition, the GPR penetration is highly influenced by the material conditions, whereas the ECT is influenced by nearby above ground conductive objects.

# GLOSSARY

### Terms, Abbreviations, and Acronyms

| | |
|---|---|
| AR | Augmented Reality |
| GPR | Ground Penetrating Radar |
| NDT | Non-destructive testing |
| ECT | Eddy Current Technology |
| EM | Electromagnetic |
| SFCW | Step-Frequency Continuous-Wave |
| AI | Artificial Intelligence |
| ML | Machine Learning |
| BIM | Building Information Modelling |
| C-BIM | Circular BIM |
| GNSS | Global Navigation Satellite System |
| EC | European Commission |
| WP | Work Package |
| WA | Work Area |
| FWI | Full-waveform inversion |
| CE | Conformité Européene (European Conformity) |
| GDPR | General Data Protection Regulation |

# TABLE OF CONTENTS

**DOCUMENT INFORMATION** ..... **3**
**REVISION HISTORY** ..... **3**
**DOCUMENT APPROVAL** ..... **3**
**EXECUTIVE SUMMARY** ..... **4**
**GLOSSARY** **5**
**TABLE OF CONTENTS** ..... **6**
**LIST OF TABLES** **8**
**LIST OF FIGURES** ..... **9**
**1. INTRODUCTION** ..... **10**
1.1. SUM4Re RESEARCH CONTEXT AND APPROACH ..... 10
1.2. SCOPE AND PURPOSE OF DELIVERABLE D2.5 ..... 10
**2. RESEARCH APPROACH** ..... **11**
2.1. STATE OF THE ART ..... 11
2.2. RELEVANCE TO THE WP2 OBJECTIVES ..... 12
2.3. RELEVANCE TO THE OTHER WP OBJECTIVES ..... 12
2.4. LEGAL CONSIDERATIONS ..... 13
2.5. TARGET MATERIALS ..... 13
2.6. CASE STUDIES APPLICATION ..... 14
**3. TECHNICAL BRIEF** ..... **16**
3.1. EQUIPMENT TECHNICAL SPECIFICATION ..... 16
*3.1.1. GPR sensor* ..... *16*
*3.1.2. ECT sensor* ..... *17*
3.2. EQUIPMENT DESCRIPTION WITH RESPECT TO APPLICATION AND UTILIZATION ..... 18
3.3. PREPARATORY MEASURES ..... 19
*3.3.1. Spanish pilot* ..... *19*
*3.3.2. Nordic pilot* ..... *19*
3.4. SAMPLING METHODS ..... 22
*3.4.1. Time allocations* ..... *22*
*3.4.2. Number of samples and sample distribution* ..... *22*
*3.4.3. Quality assurance and control measures* ..... *23*
*3.4.4. Procedure for data acquisition* ..... *23*
3.5. DEVELOPMENT OF AI MODELS ..... 24
**4. DEVELOPMENT** ..... **25**
4.1. HUMAN RESOURCES ASSIGNMENT AND ROLES ..... 25
4.2. SCHEDULING ..... 25
4.3. CRITICAL TASKS AND MILESTONES ..... 26
*4.3.1. Critical Tasks* ..... *26*
*4.3.2. Milestones* ..... *27*
4.4. SHORT SUMMARY OF RESULTS FROM CASE STUDIES ..... 27
4.5. HARDWARE ..... 27
*4.5.1. GP8800 sensor* ..... *27*
*4.5.2. PM8000 sensor* ..... *28*
4.6. SOFTWARE ..... 28
*4.6.1. GP app* ..... *28*
*4.6.2. PM app* ..... *30*
**5. CHALLENGES AND LIMITATIONS** ..... **33**
5.1. TECHNICAL CONSTRAINTS OF THE TECHNOLOGY ..... 33
5.2. TECHNICAL CONSTRAINTS OF THE PROPOSED METHODOLOGY ..... 34
**6. CONCLUSION** **35**
**ACKNOWLEDGEMENTS** ..... **36**

BIBLIOGRAPHY 37
APPENDICES 38
LIST OF APPENDICES ..... 39
LIST OF FIGURES IN THE APPENDICES ..... 40
APPENDIX A RESULTS FROM THE NORDIC PILOT ..... 41
APPENDIX B RESULTS FROM SPANISH PILOT IN JOLASTOKIETA ..... 45

# LIST OF TABLES

Table 1. GP8800 sensor technical specifications..... 17
Table 2. PM8000 sensor technical specifications ..... 18
Table 3. Human resources ..... 25

# LIST OF FIGURES

Figure 1. Spanish pilot site in Jolastokieta..... 14
Figure 2. Nordic pilot site in Svalbard..... 14
Figure 3. Foundation piles that support the timber apartment module..... 15
Figure 4. The Proceq GP8800 probe along with some of its features annotated..... 16
Figure 5. The Proceq Profometer PM8000 sensor. ..... 17
Figure 6. Horizontal view of the external apartment wall of the Nordic pilot which shows the different layers and components of the wall. ..... 19
Figure 7. Modelled geometry of the external wall as modelled in the simulations..... 20
Figure 8. Structure of the mock-up wall with the different layers next to an image of the actual sample ..... 20
Figure 9. The locations of where the grid scans were conducted on the mock-up sample with the grid paper and some of the lines annotated..... 21
Figure 10. Right internal scan: depth slice at d=12 mm depth ..... 22
Figure 11. The main interface of the GP app with the menus for signing in, connecting to the probe, the data menu and tutorials..... 29
Figure 12. Parameters need to be set in the app before starting an area scan. The box highlights the measuring presets to be chosen, whereas the circles show the buttons for selecting area scan size and spacing..... 29
Figure 13. Example of snapshot exported using the AR feature which projects the slice data on the iPad on top of the structure. ..... 30
Figure 14. Main interface o the PM app from which the probe connectivity, measurement menu and tutorials can be found..... 30
Figure 15. Example of a PM8000 line scan view which shows the signal strength for each rebar, the rebar diameter and concrete cover depth values..... 31
Figure 16. Area scan with the PM8000 as shown in the PM app with the rebars at both directions being visible. ..... 31

# 1. Introduction

## 1.1. SUM4Re research context and approach

The SUM4Re project — titled “Creating material banks from digital urban mining”—is a European research initiative funded by the Horizon Europe programme (ID 101129961). It runs from June 2024 to November 2027 and seeks to address the problem of construction and demolition waste, which is the largest waste stream in the European Union. Instead of treating this waste as a burden, SUM4Re aims to transform it into an opportunity by converting discarded materials into valuable materials that can be reused in new projects or in the renovation and repair of existing structures.

The project seeks to develop and implement methods for identifying, analyzing, and tracking construction materials, including those hidden in end-of-life buildings. By doing so, SUM4Re ensures that components with reuse potential can be recovered before demolition, thus reducing the need for raw materials and supporting the transition to a circular economy in construction. This work combines the principles of urban mining with advanced digital and technological tools, including different scanning techniques, artificial intelligence (AI) algorithms for data interpretation, circular Building Information Modelling (BIM), and blockchain technologies for material traceability. Materials banks will be built for identified reusable materials to enable traceability.

The consortium behind SUM4Re is composed of 17 partners, bringing together universities, research and technology centers, and industrial companies from across Europe and is coordinated by University of Vigo in Spain. For this project, collaboration across diverse expertise areas is needed such as engineering, sustainability, and construction management, where the multidisciplinary nature reflects the complexity of the challenge and the need for joint action between research and industry.

To demonstrate the feasibility and practical value of its approach, SUM4Re will carry out three pilot projects in different European locations, namely in Spain, in Norway and in the Netherlands, on residential, tertiary, industrial & infrastructure assets. These pilot sites will provide real-world testing grounds where the methods and digital tools developed by the project can be applied and validated.

The goal of SUM4Re is to promote circularity in the construction sector. By making the recovery and reuse of construction and demolition waste more efficient, the project will help reduce waste generation, increase the supply of secondary materials, and prioritize reuse over disposal. Equally important, the initiative promotes the adoption of open digital standards, ensuring that the solutions it develops are interoperable and scalable across Europe. In this way, SUM4Re contributes to the broader EU ambition of a sustainable circular economy.

## 1.2. Scope and purpose of deliverable D2.5

This deliverable serves to describe the progress made and results achieved for Task 2.5:

*T2.5 Data collection for complex or concealed elements with GPR-ECT (M3-M17) EAGLE; MOYUA, AFDECOM, NORSKE*

*The addition of GPR & ECT in a single device will enable material identification (metallic vs non-metallic) at rebars/concrete T10.1 and timber T10.3 as well as accurate information about dimensions of the internal components of 3D AR images obtained with GPR. This task will focus on (1) combination of GPR-ECT technologies with the following high-level product requirements: handheld compact mechanical design, accuracy-resolution compliance with all major standards, technical specs meet or exceed currently available GPR and ECT devices; and (2) development of AI Transformers Domain Adaptation (DoT) algorithms integral to GPR-ECT training for automated material detection. The best performing models for material identification will be applied to the demonstrators in WP10 in collaboration with MOYUA, AFDECOM, NORSKE.*

# 2. Research approach

## 2.1. State of the art

Ground Penetrating Radar (GPR) has evolved into one of the most flexible and widely adopted technologies for non-destructive testing (NDT). Its ability to probe beneath the surface without causing damage makes it an invaluable tool across a broad spectrum of industries. Applications range from inspecting concrete buildings and monitoring the structural integrity of bridges to mapping underground utilities, evaluating road conditions, conducting archaeological surveys, and investigating geological formations, among many others (Daniels) (Wai-Lok Lai, and Dérobert and Annan).

At its core, GPR is employed to characterize subsurface materials, detect and delineate different layers, identify hidden objects, locate anomalies, and evaluate the overall condition and structural health of materials and layers. The growing popularity and broad deployment of GPR stem from its numerous advantages: it is non-invasive, enables rapid data acquisition, and offers high spatial resolution—particularly beneficial in applications where time and accuracy are critical.

GPR functions by emitting electromagnetic (EM) waves into a target medium—commonly soil, rock, pavement, or concrete—using a transmitting antenna. These waves travel through the material and are partially reflected to a receiving antenna when they encounter boundaries between materials with differing dielectric properties. The strength and timing of the reflected signals provide information about the depth and nature of the subsurface features.

The contrast in dielectric permittivity between materials is essential for signal reflection, and this contrast forms the basis for interpreting the subsurface structure. GPR systems typically operate within a frequency range of 10 MHz to 5 GHz. Lower-frequency systems (e.g., 10–400 MHz) offer greater penetration depth, making them suitable for geological and utility applications, while higher-frequency systems (e.g., 1–5 GHz) provide finer resolution at shallower depths—ideal for inspecting concrete structures and pavements.

Since its first practical applications in the 1970s, GPR technology has seen substantial advancements. Improvements in antenna design, computational hardware, signal processing algorithms, and overall system integration have led to significant enhancements in data resolution, penetration depth, ease of use, and system portability.

Modern commercial GPR systems are often compact, lightweight, and designed for convenience. Many are handheld or mounted on carts and are integrated with Global Navigation Satellite Systems (GNSS) or total stations, enabling accurate geolocation of data. Enhanced antenna shielding has reduced vulnerability to external electromagnetic interference, improving data reliability in urban or electromagnetically noisy environments.

On the hardware side, recent innovations have enabled the development of Stepped-Frequency Continuous-Wave (SFCW) GPR systems (Solla, Novo and Elseicy), which offer improved frequency control and resolution compared to traditional pulsed systems. These systems have expanded the capabilities of GPR and are becoming more frequently used.

Whilst single-channel GPR systems remain common, recent technological advancements have led to the development of **multichannel GPR systems** (Goodman and Piro). These systems incorporate multiple antennas, arranged in arrays, enabling simultaneous data acquisition across a wider swath of ground. Also, their small channel spacing with dense data acquisition allows for capturing small features, such as small cracks, that could not be seen before with single channel systems and coarser line spacing. **Vehicle-mounted multichannel GPRs**, in particular, have revolutionised large-scale surveys. Capable of covering many kilometres in a single pass, these systems significantly reduce the time and cost required for surveying extensive areas, compared to traditional single-channel approaches which demand multiple passes.

GPR usability has also improved substantially. Wireless control of GPR systems is now common, eliminating the need for cumbersome cables and enabling remote operation through mobile devices such as tablets. Some systems can now be operated entirely via an iPad app. Real-time features have also advanced considerably—field operators can now generate and view time/depth slices directly on site, overlay radar data on background maps, and track their position visually during the survey.

GPR data collection methods vary depending on whether a positioning system is used. In surveys without GPS or GNSS, operators typically lay out a structured grid and collect data along parallel lines

in two orthogonal directions. In contrast, when a positioning system is used, data can be collected freely, with spatial coordinates automatically recorded.

Raw GPR data are typically visualized as B-scans, which are 2D radargrams showing signal amplitude as a function of depth (vertical axis) and distance along the survey line (horizontal axis). From multiple parallel B-scans, time/depth slices—plan-view representations of subsurface reflections at specific depths—can be generated to provide a more understandable images and understanding of buried features.

Basic data processing is often possible through the GPR system's onboard or acquisition software, but advanced analysis typically requires dedicated post-processing software. These are provided either by equipment manufacturers or third-party developers, offering tools for filtering, migration, amplitude correction, and other signal enhancements.

In addition to hardware evolution, significant progress has been made in GPR data processing and interpretation. Advanced processing methods, such as 3D migration, reverse-time migration, full waveform inversion (FWI), and wavelet analysis, have been implemented to improve the accuracy and clarity of subsurface imaging. Furthermore, artificial intelligence (AI) and machine learning (ML) techniques are increasingly being used—for instance, for automatic detection of rebars in concrete (Elseicy, Solla and and Novo) (Faris et al.) and material characterization (Patsia, Giannopoulos and & Giannakis)—reducing manual effort and increasing consistency in interpretation.

Modelling capabilities have also improved dramatically. Modern EM numerical simulation tools enable the creation of complex 3D models that include realistic representations of antennas, heterogeneous materials, and irregular geometries (Warren, Giannopoulos and & Giannakis). These models make it possible to simulate real-world survey scenarios, generate synthetic radar data, and assess system performance under various conditions. This capability is invaluable for system testing, training, and enhancing interpretation strategies in actual field data.

## 2.2. Relevance to the WP2 objectives

Work package 2 (WP2) aims to develop a set of different efficient methods to locate and characterise materials from end-of-life buildings that can be reused. Each of these methods will contribute by providing different information regarding a material's condition.

Task 2.5 directly supports the WP2 objectives as it offers the methodological framework on how to efficiently conduct a GPR + ECT survey, data collection and analysis in concrete and timber-based buildings for characterising materials and finding hidden elements. In particular, with the GPR sensor, structural or other hidden elements (e.g. reinforcing bars, wooden studs, pipes, insulation etc.) inside walls and floors can be identified, information can be acquired regarding the internal condition of materials (e.g. wet vs dry concrete) in addition to detecting voids and cracks in a structure. With the ECT technology, the concrete cover depth is estimated, rebars are located along with their diameter estimation and also rebar corrosion. Both are two matured technologies that can be used together to identify reusable components and materials and therefore align with the goals of WP2.

This task will describe the technology and methodology followed from data collection to results presentation, as well as the understanding of the limitations of each method and present case studies to demonstrate the methodology in practice.

The information from the GPR and ECT results can be used complementary to the results from the other technologies in WP2 to make conclusions on the condition of materials and building structure. In addition, it can be used in conjunction with the external scanning techniques to provide information about the external and internal structure of a building.

## 2.3. Relevance to the other WP objectives

Task 2.5 serves as the basis of the methodology for data collection with GPR and ECT technology and is related to the following tasks:

- **WP3**. Specifically, task T2.5 is related to T3.5 where the GPR data provided in this task will be used to develop and validate generated AI models. It is also relevant to T3.7 where the sensor data will be integrated in GENIA for a subsequent development of a C-BIM structural model.
- **WP10**. The methodological framework developed in task T2.5 is necessary for the GPR-ECT data acquisition and analysis in two of the three case studies; the Nordic and the Spanish pilot site.

## 2.4. Legal considerations

One of the legal requirements for GPR technology is the equipment certification. GPR uses radio frequencies which are regulated by governments of each country and thus the equipment needs to comply with the regulations imposed by the country where it is used and hold the appropriate certification. There are different regulations in each country, such as the FCC in the United States or ETSI EN 302 066 in the EU, but for most it must use low power and operate in close proximity to the ground to limit interference. Furthermore, in the EU, the devices need CE marking to be legally sold and used.

GPR sends and receives EM signals from objects mainly in the subsurface or hidden in a structure but can also detect above ground/surface features. Since it is a radar system that can interfere with other electrical devices, another legal consideration is related specifically to the use of GPR near critical infrastructure as there might be national security or safety restrictions for its use close to airports, railways and other sensitive sites. Similarly, the ECT sensor generates magnetic fields and thus it can also interfere with surrounding electrically conductive objects.

Regarding workers' health and safety, safety measures should be taken before conducting a GPR and ECT survey and perform the necessary risk assessments. Also, the equipment should be operated only by trained operators to mitigate safety risks and avoid misuse of the technology.

The results of a GPR and ECT survey are generally considered the property of the commissioning party, but contracts should clarify ownership and establish the terms for data access and/or use by all parties. While the sensors do not capture personal information directly, in some cases an account with personal information is required to login and control the data acquisition and processing software. This information is not processed and will not be included in the BIM models as only GPR and ECT data and interpretation will be transferred to BIM, however, careful consideration under the General Data Protection Regulation (GDPR) must be given.

The data, apart from being stored locally in the iPad device, are also transferred to the cloud when internet connectivity is available. In addition, the devices mostly commonly are controlled wirelessly via Wi-Fi which can pose a risk in Wi-Fi denied areas. However, in these cases, offline versions of the data acquisition software can be used which do not upload the data to the cloud and the connection to device is performed with a cabled connection.

No other legal considerations have been identified related to the GPR and ECT technologies.

## 2.5. Target materials

GPR and ECT can be used to scan and locate different common materials used in the construction industry. One of their main applications is finding structural components in concrete such as rebars and post-tensioning cables and give information regarding their condition (e.g. corroded, cut or bent) as well as the concrete condition (e.g. the moisture content). This can help in selectively cut or deconstruct concrete to recover steel or reuse concrete blocks. For timber buildings, apart from finding hidden components inside the timber structure such as wooden studs, or insulation layers, moisture or voids could also be detected with GPR. Other potentially reusable elements that can be identified include utilities, both metallic and non-metallic, heating elements and others found typically internally in walls and flooring. In general, GPR can scan a variety of materials and identify different layers and components and thus is not limited to only concrete or timber.

Specifically for the Spanish pilot, with the GPR and ECT sensor, it is sought to locate and characterise metallic reinforcing bars hidden in concrete slabs and to acquire information regarding the condition of the concrete itself such as moisture content or the presence of voids.

From the Nordic pilot, the condition of the timber is to be identified, such as its moisture content, and the presence of cracks and voids but also to identify the wooden studs inside walls and floors. In addition, the insulation layers consisting of either glass wool, stone wool or wood fibre will be identified and characterised. Other elements hidden inside the walls and floors such as heating elements or cables will also be sought.

**Figure 1. Spanish pilot site in Jolastokieta**

## 2.6. Case studies application

To evaluate the project's proposed GPR + ECT methodology, two of the three case studies of the project were selected; the first pilot site is located in Longyearbyen, Svalbard (Norway) and the second one in San Sebastián (Spain). Each site has different materials and structures, but both are representative of construction technology in European countries.

The Spanish pilot site consists of two buildings located in San Sebastian in the Basque country of Spain; the Anoeta train station and the Jolastokieta building, from which the Jolastokieta building was scanned with GPR-ECT technology. This building is an abandoned industrial factory where elevators used to be manufactured and mainly consists of concrete with hidden metallic reinforcing structural elements. The floors are concrete slabs with a layer of mortar on top and hidden metallic rebars, whereas the walls consist of bricks and concrete without any reinforcing elements inside. The Jolastokieta building today is empty and exposed external steel beams could also be seen at the site. More information regarding the Jolastokieta pilot site can be found in the D10.1 deliverable. A picture of the interior of the building can be seen in Figure 1.

**Figure 2. Nordic pilot site in Svalbard**

The Nordic pilot site is in Longyearbyen, Svalbard which is the northmost inhabited place in the world. This is a two-floor timber-based residential building that lies on foundation piles which are placed in the permafrost layer. The walls consist of different layers including cladding, asphalt panels, insulation

layers and fibre board. The floor structure is mainly wooden with insulation layers whereas tiles can be found in the bathroom. Due to the remote location of this site, where material transport is difficult and costs are high, the material circularity is quite important. Due to the extreme weather conditions and climate change affecting the permafrost, the building supports become unstable, and this is one of the reasons this building and other buildings of a similar type were chosen to be demolished. An image of the Nordic pilot site external building can be seen in Figure 2, whereas Figure 3 shows the foundation piles under the building modules. More information about this case study is available in the D10.3 deliverable.

**Figure 3. Foundation piles that support the timber apartment module**

# 3. Technical brief

In this chapter, the technical description of the scanning equipment used is provided. Two systems were used: 1. The Proceq GP8800 GPR probe and 2. the Proceq Profometer PM8000 ECT sensor. For the Spanish pilot, both sensors were used whereas for the Nordic pilot, only the GPR sensor could be used.

## 3.1. Equipment technical specification

### 3.1.1. GPR sensor

For the GPR scanning, the Proceq GP8800 GPR sensor was employed. This sensor is a step-frequency continuous-wave (SFCW) system with a modulated frequency range of 400–6000 MHz. With its modulated frequency and compact antenna, the GP8800 is considered a high-frequency GPR system. This means it provides high resolution, making it capable of detecting relatively small subsurface features at shallow depths. Its maximum penetration depth is around 65 cm, which can vary depending on the material conditions of the surveyed area. Higher moisture content can reduce a system's penetration capabilities.

The GP8800 is a single-channel system and includes two antennas: a transmitter (Tx) and a receiver (Rx), both housed in a single case. The probe has a compact design, measuring just 8.9 x 8.9 x 7.6 cm and weighing approximately 500 grams, making it lightweight and easy to use in the field. Its operating temperature range is between 5° and 40°C. Additionally, the system is equipped with a replaceable skid plate, which helps to protect the antennas from damage during scanning.

This system also features an adjustable wheel, which not only serves as a distance encoder but also enables the system to operate in both normal and cross-polarization modes by adjusting the wheel position. The choice between these two modes depends on the type of subsurface features being targeted, as each mode offers better detection of specific materials or objects.


**Figure 4. The Proceq GP8800 probe along with some of its features annotated**

In terms of powering the GP8800, there are several flexible options. The system can be powered by a removable Lithium-ion battery pack with 8 hours autonomy, a set of four AA (NiMH) batteries, or an off-the-shelf 10,000 mAh power bank. This allows users to select the most convenient or available power source depending on the duration and location of the survey.

The sensor is controlled using an iPad application called the GP app, which connects either wirelessly to the sensor via Wi-Fi or through a USB-C cable. The app not only provides control over the system for data acquisition but also allows for real-time data visualization and basic signal processing directly on-site. When an internet connection is available, the app allows users to upload the data to the cloud, where these are stored on the Workspace platform.

The GP8800 system is designed to operate in direct contact with the surface being scanned, whether it is the ground, concrete walls, or other surfaces, to ensure the maximum penetration of the radar signals. The primary application for this system is in concrete inspection, where it is used to locate key structural elements, including rebars, post-tension cables, and conduits but also to characterize concrete itself. The system is also utilized for other high-resolution applications, such as wooden pole inspections and any scenarios where high resolution is required for the detection of subsurface features. An image of the GP8800 system is shown in Figure 4 below, and some of its technical specifications are summarized in Table 1.

**Table 1. GP8800 sensor technical specifications**

| Feature | GP8800 |
|---|---|
| **Radar technology** | SFCW GPR system |
| **Modulated frequency range** | 400 – 6000 MHz |
| **Penetration depth** | 65 cm |
| **Dimensions** | 8.9 x 8.9 x 7.6 cm |
| **Weight** | ~500 g |
| **Charging** | Li-ion Battery Pack: Up to 8 h<br>Battery Pack (4xAA NiMH): Up to 2.5 h<br>Power bank (not included): Up to 8 h |

### 3.1.2. ECT sensor

For the ECT scans, the Proceq Profometer PM8000 was employed as the sensing device. This instrument operates on the principle of electromagnetic induction, utilising a series of coil configurations that generate magnetic fields when excited by short electrical pulses. The interaction between these fields and nearby conductive materials produces eddy currents at the material's surface. In the context of reinforced concrete structures, these currents are induced specifically in the embedded steel rebars. Through this non-destructive mechanism, the PM8000 can locate rebars, estimating cover depth, and determining rebar diameter with considerable precision. The Profometer performance is validated both during the instrument manufacturing and testing process before deployment but also before conducting a survey using reference reinforced concrete blocks to ensure the accuracy of the cover and diameter estimates. The accuracy for the cover depth is +/-1 mm to 4 mm depending on depth and up to 185 mm with +/-1 mm accuracy provided up to 80 mm depth, whereas for the rebar diameter is +/- 1 rebar size which holds up to 63 mm rebar depth.

The performance of the ECT sensor is influenced by the position of the reinforcement. When rebars are located close to the concrete surface, the system can measure their diameter with high accuracy for up to a depth of approximately 6 cm. However, the accuracy for diameter estimation is reduced beyond that depth. For cover depth estimation, the profometer achieves reliable measurements at greater penetration depths, up to around 16 cm, depending on the conditions. These capabilities make it particularly valuable for assessing existing reinforced concrete structures where precise information on reinforcement layout and dimensions is required.

**Figure 5. The Proceq Profometer PM8000 sensor.**

From a practical viewpoint, the probe is designed for portability and ease of use. The sensor unit with its encoder cart measures 25 × 13 × 4.5 cm and weighs 690 grams, making it compact enough for field applications. Figure 5 illustrates the PM8000 sensor attached to its encoder cart. The device is powered

using either a pack of two AA NiMH batteries—rechargeable or disposable—with an autonomy of up to 8 hours, or alternatively via a USB-C power bank, ensuring continuous operation during extended site investigations. Some of its technical specifications are summarized in Table 2.

Similar to the GPR system, it is controlled through an iPad interface using the dedicated PM app. This application enables operators to manage data acquisition, perform real-time visualization, and conduct basic on-site data processing. Moreover, the app includes cloud upload features to the Workspace platform, allowing collected data to be uploaded, stored, and shared for further analysis or collaboration. This digital integration enhances the efficiency of inspections and facilitates data management.

**Table 2. PM8000 sensor technical specifications**

| Feature | PM8000 |
|---|---|
| **Technology** | ECT system |
| **Cover depth measurement** | Up to 180 mm |
| **Rebar diameter measurement** | Up to 63 mm |
| **Dimensions** | 250 x 130 x 45 mm (with cart) |
| **Weight** | ~690 g (with cart) |
| **Charging** | 2 x AA (NiMH) rechargeable or not and removable with 8h autonomy USB-C power bank |

## 3.2. Equipment description with respect to application and utilization

The GPR sensor was used in the San Sebastian pilot to scan both walls and floors. This is a reinforced concrete structure which requires a high-resolution GPR system for locating the reinforcement and other hidden elements and characterising the concrete itself and does not require large penetration depth. As this is the main application of the GP8800 system, this probe was the perfect choice for this pilot site.

The ECT PM8000 sensor was employed on the floors of the San Sebastian pilot where rebars were included in the floor structure. One of the requirements was the identification and characterization of the rebars in concrete, justifying the use of this sensor, which is used for rebar detection, rebar diameter estimation and concrete cover depth estimation. This probe could not be used on the walls of the Spanish pilot as no metallic reinforcement was present.

For the residential building in Svalbard, the GPR sensor was used for scanning walls internally and externally and floors to identify hidden structural elements (e.g. wooden studs, joints, beams), detect different interior layers and their condition as well as the timber condition. Although the GP8800 probe was initially designed for concrete scanning, it can be used for other materials as well such as timber as GPR can penetrate timber and “see” the internal structure. Applications of GPR for wooden utility poles or other tree trunks can be found in the literature.

The high-resolution of the GP8800 system allows for detecting small internal features such as cracks if present. The PM8000 could not be used in the Nordic pilot, as an ECT sensor requires electrically conductive elements to be present and this is a timber structure with no metallic reinforcement inside. Since both sensors are small and lightweight, the portability of the equipment is not an issue in such a remote location as Svalbard.

For both cases studies, the depths of hidden elements and the thickness of layers can be estimated. Both the GPR and ECT sensors offer rapid and dense data collection, portability due to their small weight and give information on the internal structure which can complement the techniques which provide only surface information. In addition, due to their small size, they allow for easy scanning close to wall corners found in buildings. Since both are NDT methods, they allow for inspection without the need for destruction of the structure.

## 3.3. Preparatory measures

Multiple preparatory measures were taken before visiting the pilot sites for data acquisition to ensure efficient and smooth scanning, reliability of the data and results and minimize risks that might occur on-site.

### 3.3.1. Spanish pilot

First, the survey objectives were defined. This is necessary as the GRR system is chosen based on the survey objective in order to provide the required depth and resolution. In addition, photos and existing information of the Jolastokieta site were studied to maximize the understanding of the structures and plan the survey setup and scanning locations better.

Regarding visiting the site, coordination with MOYUA was done beforehand to decide the scanning dates, secure the necessary site access permit and make early travel arrangements.

No previous testing on similar structures was necessary in this case as both the GPR and ECT have been widely used for scanning different concrete slabs under different conditions (e.g. wet vs dry, with or without voids, with different types of reinforcement) and the data have been studied well.

### 3.3.2. Nordic pilot

Similarly to the Spanish pilot, first the goals of the survey were listed and information on the apartment building was studied. This included drawings of the apartment layout, external and internal photos of the site and the available information on the materials that the walls and flooring are composed of as well as the different layers. This assisted in deciding both the scanning locations and the density of the samples needed.

For accessing the building, the scanning dates and travel arrangements were decided after coordination with SINTEF and STORE NORSKE, where the latter also provided access to the building site.

Since scanning a timber-based building is not a common GPR application some additional preparatory measures were taken to acquire a better understanding of the GPR propagation in this type of structure, ensure smooth survey and assist in the interpretation of the field data. The first measure was to conduct simulations whereas the second measure was to perform scans on a mock-up sample which is a smaller version of the exterior walls found in the apartments of the timber building.

Simulations were conducted in the open-source software gprMax which is a finite-difference time-domain (FDTD) solver. A drawing with the structure of the external wall was provided and based on this, a full 3D model of the external wall was created with all the layers and true dimensions being modelled. The structure of the wall can be seen in Figure 6, where the different layers can be seen with the main ones being the cladding, asphalt panels, insulation and fibre board. In addition, the wooden studs present inside the wall can be seen. The modelled geometry included in the simulations can be seen in Figure 7.

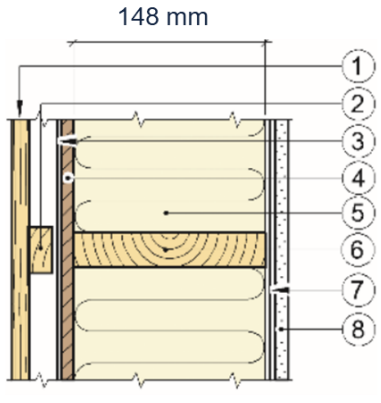


Horizontal view of outer wall

1. 19x148 mm horizontal double-beveled cladding with two layer of system coat
2. 23x48 mm battens/ventilation
3. Wind barrier
4. 12 mm windproof asphalt panels
5. 150 mm mineral wool insulation
6. 36x148 mm studs, spaced 600 mm center-to-center
7. 0.15 mm plastic film/vapor barrier
8. Medium/high density fibre board beveled paneling (laminated chipboard in storage rooms)

**Figure 6. Horizontal view of the external apartment wall of the Nordic pilot which shows the different layers and components of the wall.**

As for each of the materials present in the wall, their exact dielectric properties were unknown, common values for these types of materials were used in the simulations. For a layer/object to be detected with

GPR, a dielectric contrast needs to exist between the object and its surrounding material or between a bottom layer and the top layer. The greater this difference in dielectric properties, the stronger the signal that will be received.

It was found that although the different materials present in the wall have small dielectric contrasts between them, there are still some layers and hidden elements that can be easily detected even with minimum post-processing such as the wooden studs inside the wall. This is only what is expected theoretically and was further verified with the scans conducted in the mock-up sample.

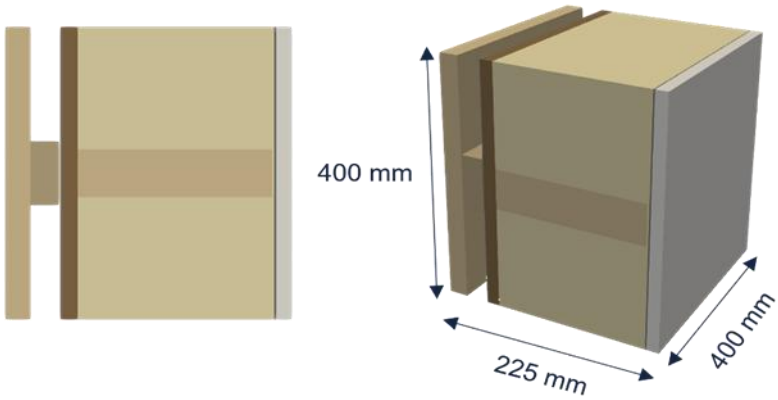


**Figure 7. Modelled geometry of the external wall as modelled in the simulations**

Prior to the Svalbard testing, a mock-up wall sample was constructed and scanned using the GP8800 sensor to verify the theoretical results in practice and determine which information can be extracted from this structure, to plan the scanning setup better and finally assist in the interpretation of the field data from Svalbard. A photo of the mock-up sample along with a drawing of its structure is given in Figure 8. The sample has dimensions of 1200 × 800 × 211 mm.

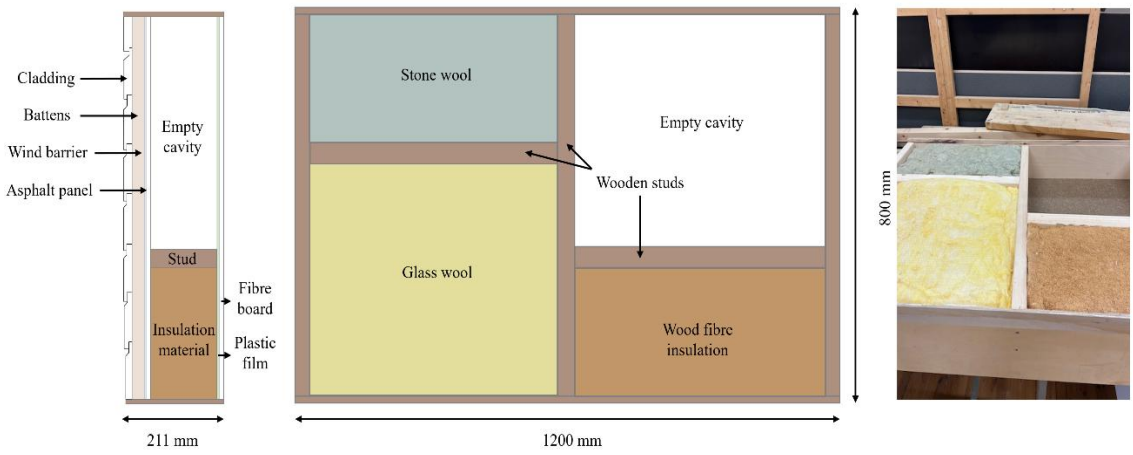


**Figure 8. Structure of the mock-up wall with the different layers next to an image of the actual sample**

Since this is a specimen of known thickness, it was used to acquire bulk estimates of the dielectric/velocity values through the medium which are needed for accurate depth estimations of objects and layer interfaces. While performing the scans, the response from the backwall can be seen as a flat response and since the depth is known, it can be set and thus used to calibrate the dielectric. Ideally, since each layer has different properties, different dielectric values should be used for each layer; however, it is common in practice to use a bulk value that represents the whole medium. For the region with the empty cavity, the dielectric was estimated to be $\varepsilon = 1.3$ since this section is mostly air and EM waves travel faster through air than through other media. For the insulated regions, the dielectric was estimated to be $\varepsilon = 2.5$. However, this is a dry specimen and thus these values can be different in the actual building wall which may also be affected by moisture.

The sample was scanned from both the external cladding and the internal fibre board side. Two 60 × 60 cm grid scans were performed on each side with some overlapping between the two scans, resulting in 4 grid scans in total. Scanning from both sides was performed since one of the requirements is to also conduct scans external to the building. Each area and all lines were marked with a grid paper. Two grid scans were needed on each side to ensure that the full sample is scanned. For each area scan, lines were collected both in the x and y direction with a dense spacing of 5 cm, resulting in 26 measurements in total. Figure 9 shows an image of the sample from the external cladding side along with the area scan locations.

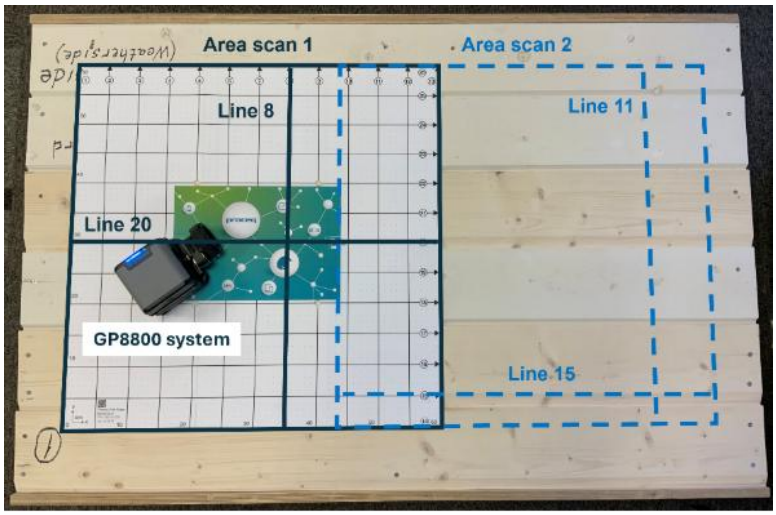


**Figure 9. The locations of where the grid scans were conducted on the mock-up sample with the grid paper and some of the lines annotated.**

The scans were performed by starting with the x direction followed by the y-directed scans. After the data were collected, certain processing filters were applied in order:

1. Time zero correction: This filter shifts the GPR data upwards by a certain number of samples for the 0 m to represent the ground surface. Time zero correction is necessary as it is used to correct depth estimation and is usually the first filter applied in all GPR data.
2. Noise cancellation filtering: Used for removing noise from Wi-Fi or cellphones that might be present in the data.
3. Background removal: This filter is used to remove banding noise from the data which appears as along horizontal stripes. In addition, it is used to remove the direct wave response (direct air + direct ground wave) which due to its strong signal, masks other shallow responses. In this case, this filter was applied only to a time window to avoid removing other responses from interfaces or the backwall.
4. Gain: Signals get weaker with depth and thus deeper responses might be faint or not visible. Gain is used to amplify the data and make deeper responses visible. An automatic gain was used in this case, which calculated automatically a gain curve based on the signal strengths of the data.

Each line collected from an area scan is presented as an image called a radargram or B-scan. After all lines have been collected, the data are combined in a volume from which time/depth slices can be cut to show the data at specific depths. One example can be seen in Figure 10 where the depth slice at d=12 mm depth is displayed in which the responses from the middle and side wooden studs can be seen.

From the data analysis, it was determined that in addition to the wooden studs, the insulation/asphalt panel interface and the cladding/air interface could also be detected. In addition, the transition between the empty region and the insulated regions could be observed in the data and thus detect material changes. More results and details from the mock-up scans can be found in deliverable D10.3.

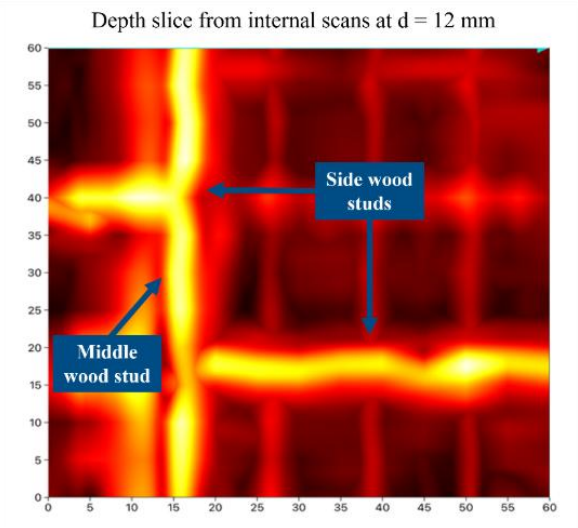


**Figure 10. Right internal scan: depth slice at d=12 mm depth**

## 3.4. Sampling methods

### 3.4.1. Time allocations

At each pilot site, an initial 30-40 minutes period is required for observation of the building to get a better understanding of the structure and acquire information that might be useful for the data collection and interpretation but also for identifying any possible challenges and limitations that had not been accounted for beforehand.

For each 60 x 60 cm dense area scan approximately 20 minutes are needed for setting up the control application, the grid paper, position the sensor and performing the data collection with the GPR sensor. A similar amount of time is required for the initial calibration of the ECT sensor and the data collection for the same size of area and spacing. The full data collection in the Nordic pilot took approximately 8 hours, whereas in the Spanish pilot site, it took 4 hours.

After data collection, a quick 1-hour post-processing and checks were carried out on-site to check the data quality, ensure there were no issues with the data collection process and to create data back-ups.

At a later stage after the visit to the site, the full post-processing of the data will be performed which typically requires 4-5 times the amount of time needed to conduct the data collection. This time also includes the time needed for creating the exports of the results. However, specifically for the Nordic pilot, since this is a more complex application, it was estimated that more time will be required for data analysis. The processing of the Svalbard dataset took approximately 8 days, whereas for the San Sebastian dataset, 3 days were required in total.

### 3.4.2. Number of samples and sample distribution

The number of samples required depends on the variability of a structure. If most sections of a building have the same structure, then fewer samples are required as these few samples are considered representative of the total area. However, if high variability is observed, then more samples are needed at different locations to capture this variability and acquire as much information as possible.

For the Nordic pilot, GPR data were collected at 24 different locations due to the differences found in the structure at the different areas of the two apartments (first and second floor apartment). Specifically, these scans were conducted at:

- Internal walls between rooms of the same apartment
- Internal wall between two apartments
- External walls (scanning from the internal side)
- Floor over foundation
- Floor of the second-floor apartment
- Floor of two different rooms
- On the external wall section between the first and second floor. Specifically, on the area in-between the windows of the lower and upper apartment.

- On the side wall of the balcony
- External scans performed on the cladding side.

In contrast, for the Spanish pilot, only 4 areas were scanned first with the GPR sensor and after with the ECT probe, as these areas were representative of the conditions found in most of the building structure. Scans were performed at:

- The driest concrete floor slab observed which included reinforcement
- Wet floor concrete slabs which included reinforcement
- Wall which did not include reinforcement

In most cases, an area of 60 x 60 cm was scanned, apart from one case at each pilot size, where due to size limitations a 40 x 40 cm area was scanned. A spacing of 5 cm was chosen between lines whereas for each individual line, samples were collected at a rate of 2 scans/cm for dense data collection and high-resolution. This resulted in a total of 26 lines for each 60 x 60 cm grid, and 18 lines for the 40 x 40 cm grids.

### 3.4.3. Quality assurance and control measures

Prior to visiting the survey area, it is crucial to ensure that the necessary equipment is fully functional. Thorough equipment checks should be performed such as verifying that batteries are charged, there is connectivity to the system, GPR antennas are working as expected and data look correct. These checks should also be performed at the field, before starting the data collection. All the necessary checks were conducted prior to data collection at each site.

Since the survey area can be at a remote location, it is essential to have spare battery packs, chargers and even additional GPR systems if possible. Having backup equipment ensures that the survey won't be delayed in case of break downs. For the Nordic pilot, two units of the GP8800 system were transported along with two battery packs and chargers. Two iPads with the acquisition software were also available. Similarly for the Spanish pilot, however, in this case, two units of the Profometer ECT sensor were also transported to the site in addition to the GP8800 systems.

The site surface preparation also plays a crucial role in the quality of the GPR survey. The surface of survey area should be cleared of obstructions, such as debris, metallic or other objects (e.g. furniture in the Nordic pilot building), in order to minimise signal distortion.

In addition, it's important to log and document survey parameters such as spacing, number of lines, photos of survey area, as well as any changes in the survey approach. This detailed documentation supports the integrity of the data and helps for future reference or replication of the survey. This was done in the acquisition apps which store all these parameters and provide the option of attaching photos, notes and voice recordings to the measurements.

In addition to equipment, operator training is essential for ensuring the quality of a GPR survey. Only experienced and trained operators should conduct the survey, as they are more likely to correctly handle the system, understand the data collection, and make informed decisions about equipment settings and survey techniques. All operators who performed the data collection in both sites are highly experienced.

To ensure there is no data loss, it is essential to regularly back up the data to multiple storage devices (such as external hard drives or flash drives) or/and to cloud storage when there is internet connectivity available. Apart from storing the data locally on the iPad, the data were also uploaded to the cloud in the Workspace platform and shared among the different operators as an additional backup.

### 3.4.4. Procedure for data acquisition

For both the GPR and the ECT technologies, the process followed was the same. The procedure for data collection starts by laying out and securing the grid paper to mark the scanning area and position of the measurement lines. If needed, before this step, obstacles are removed, and the surfaces are cleaned of debris first. The system is powered up and connected to the acquisition application either wirelessly (via Wi-Fi or Bluetooth) or using a cable.

Once the connection is established, the user needs to create a new measurement and select the scanning settings such as mode, area size and repetition rate. Once the necessary settings are chosen, data collection can be initiated. The starting point is marked on the grid paper with 0, 0 and lines are collected one at a time starting from the x direction. When all x-directed lines have been collected, scanning in the y-direction is performed. Scanning in both directions, although not necessary, is recommended as different elements can be detected better in the one direction from the other. Any line

can be recollected if necessary. During the collection, each line data can be visualized live on the app and basic processing can be applied. In addition, for the GPR data, the time/depth slices are also created and can be visualized live. If there are features of known depth or thickness, these can be used for in-situ dielectric/depth calibration which was performed in Svalbard where the wall and layer thickness was known. However, in cases where this information is not available such as the Spanish pilot case, a process called hyperbola fitting can be used to acquire estimates if a hyperbola is present in the data.

Photos of the scanning locations are taken using the app with the option to write comments and record voice notes. Operators can also add virtual markers in the data to mark features of interest onto the data. For the GPR slice data, the available AR feature can also be used to project the data directly to the survey area.

After the data collection is finished, when internet connectivity is available, the data are synced to the cloud and stored in the Workspace platform.

### 3.5. Development of AI models

An AI model is currently being developed to perform material characterization from GPR data, as part of project tasks T2.5 and T3.5. The objective is to enable automatic estimation of material properties from radar measurements, enhancing both interpretation accuracy and processing efficiency. To achieve this, the AI model will be trained primarily on synthetically generated data that closely replicates real-world GPR signals. Ensuring the resemblance of the synthetic data is critical; therefore, considerable effort is devoted to accurately modelling the physical and electromagnetic characteristics of the system. This includes detailed representation of:

- The EM properties, heterogeneous composition and complexity of materials (e.g., soil, concrete, moisture content)
- The geometry of the background media and embedded hidden objects
- The antenna system and its excitation waveform.

Accurate modelling of all these aspects is essential, as any simplification or inaccuracies could lead to synthetic data that deviates significantly from real measurements, thereby reducing the AI model's generalization capability.

For generating the synthetic dataset, a 3D Finite-difference time-domain (FDTD) electromagnetic solver is used (Warren, Giannopoulos and & Giannakis). This solver numerically solves Maxwell's equations, allowing the simulation of complex EM wave interactions within the subsurface. The numerical modelling approach was selected because it enables the generation of large and diverse datasets—covering thousands of scenarios—reducing significantly the time and cost required for extensive field measurements. Furthermore, synthetic data provide full control over the ground truth, including exact material parameters and object properties, which are typically difficult or impossible to determine from real-world data with high precision.

The AI framework utilizes a regression-based ML model, implemented using neural networks, to predict material parameters from GPR signals. Initially, the network will be trained exclusively on the synthetic dataset and interpreted data from the two pilot sites will be incorporated for testing and fine-tuning. Afterwards, these can be included to the training set—combining synthetic and real data—in order to improve model robustness and adaptability to real-world conditions.

ML scripts and the overall processing pipeline have already been developed and are currently awaiting full-scale training and validation pending required optimization of the simulations. Future work will focus on iterative training, cross-validation, and performance benchmarking using both synthetic and real datasets to ensure reliable predictions.

# 4. Development

## 4.1. Human resources assignment and roles

**Table 3. Human resources**

| | Affiliation | Role | Contact info (mail) |
|---|---|---|---|
| **Alex Novo** | EAGLE | Supervision and GPR + ECT data collection | alex.novo@screeningeagle.com |
| **Ourania Patsia** | EAGLE | GPR + ECT data collection + analysis | ourania.patsia@screeningeagle.com |
| **Rosaly Wiegmans** | EAGLE | GPR + ECT data collection | rosaly.wiegmans@screeningeagle.com |
| **Sveinung Nesheim** | SINTEF | Support related to the built environment (geometry/materials) and objectives of each case study. | sveinung.nesheim@sintef.no |
| **Ramon Hingorani** | SINTEF | | ramon.hingorani@sintef.no |
| **Jon Zubizarreta** | MOYUA | | jon.zubizarreta@etra.eus |
| **Anders Lundli** | AFDECOM | | anders.lundli@afgruppen.no |
| **Emil Lindberg** | NORSKE | | Emil.lindberg@snsk.no |

## 4.2. Scheduling

T2.5.1 Design basis of methodology (M3 to M7)

T2.5.2 Development of simulations and analysis (M8 to M10)

T2.5.3 Data collection on mock-up sample and conference paper writing (M10 to M11)

T2.5.4 Preparations for data collection in pilot sites (M11 to M12)

T2.5.5 Data Collection in Svalbard and analysis (M13 to M14)

T2.5.6 Data Collection in San Sebastian and analysis (M14 to M15)

T2.5.7 Report writing and review (M14 to M17)

| | 2024 | | | | | 2025 | | | | | | | | | |
|---|---|---|---|---|---|---|---|---|---|---|---|---|---|---|---|
| | Aug | Sep | Oct | Nov | Dec | Jan | Feb | Mar | Apr | May | Jun | Jul | Aug | Sep | Oct |
| | M3 | M4 | M5 | M6 | M7 | M8 | M9 | M10 | M11 | M12 | M13 | M14 | M15 | M16 | M17 |
| T2.5.1 | | | | | | | | | | | | | | | |
| T2.5.2 | | | | | | | | | | | | | | | |

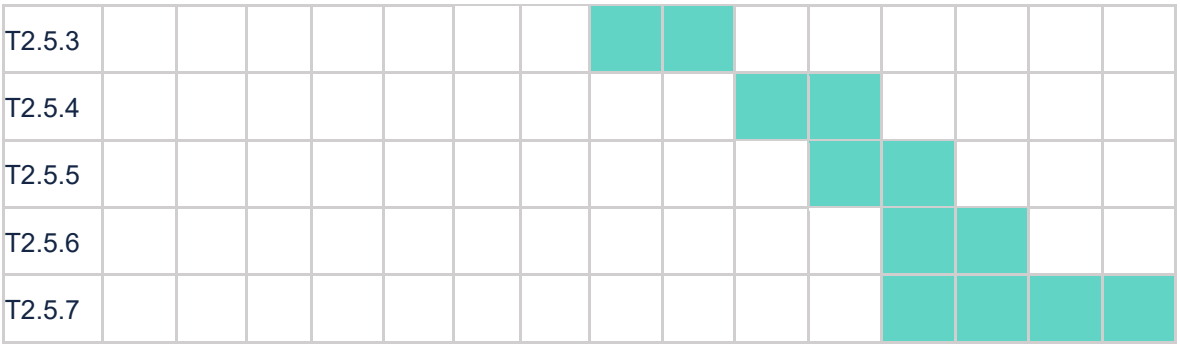


## 4.3. Critical tasks and milestones

### 4.3.1. Critical Tasks

| Critical Task 2 | Probability | Impact |
|---|---|---|
| Different testing materials are not available for verification due to logistics | Med | Med |
| **Contingency** | | |
| Investigated materials will be decided before testing and distributed to all participants in due time. | | |

The investigated materials were identified beforehand by each case study managers (MOYUA, AFDECOM, NORSKE). Drawings, plans and images of the pilot sites were given to acquire more information on the materials of each case study. Data acquisition in each pilot site went smoothly.

| Critical Task 3 | Probability | Impact |
|---|---|---|
| The contamination of the samples for analysis might affect to the accuracy and reliability of the data | Low | High |
| **Contingency** | | |
| Implementation of tailored protocol for the sample handling, preparation, and analysis. Regular cleaning and maintenance of the XRF equipment. | | |

Not applicable.

| Critical Task 4 | Probability | Impact |
|---|---|---|
| The processing of huge amounts of raw data (e.g., AHS, XRF) can lead to incorrect conclusions | Low | High |
| **Contingency** | | |
| Develop and implement an automated data pre-processing by skilled data scientists with experience in handling large datasets. | | |

Given the mock-up scanning results, the simulations and prior experience of skilled scientists with a variety of different applications and large datasets (including multiple kilometres of data with hundreds of GBs size), careful data analysis and efficient processing recipes were implemented to ensure correct interpretation and conclusions are made.

| Critical Task 5 | Probability | Impact |
|---|---|---|
| Technical limitations or malfunctions in the equipment (i.e., AHS, XRF) could lead to incomplete or erroneous data collection | Low | High |
| **Contingency** | | |
| Regularly maintenance and calibration of the equipment to ensure optimal performance and accuracy. Additionally, a backup of the equipment available in case of any technical failure. | | |

Both the GP8800 and the PM8000 sensors are regularly checked with firmware updates and app updates being also regularly made. New battery packs with 8h autonomy were used and a backup sensor was available for both systems in the field, ready to be used in the case of any technical failure of the primary units.

#### 4.3.2. Milestones

- AI models for material detection in the field (M17)

Verification form: Algorithms and laboratory results (D2.1 to 2.6) completed.

D2.5 (together with the other WP2 deliverables) ensures that there is sufficient data on which to train and test the WP3 AI algorithms. Thus, the complementation with open datasets ensure the smooth operation of WP3 and of the project.

## 4.4. Short summary of results from case studies

From the GPR scans conducted in the Spanish pilot with the methodology presented here, the reinforcing mesh in the concrete floor slab could be detected and located along with other observed linear features which are possibly different types of reinforcement or pipes. In addition, in certain locations, small features of irregular shape could be observed which could potentially correspond to voids.

Overall, the concrete slab had a high moisture content which could be confirmed by the high dielectric values of 9-12 (typical values for wet concrete) but also from visual observations of the surface. Additionally, there was a shallow layer observed in the data which included weaker and stronger amplitude regions. Although the ECT scans were also performed, the depth of the rebars exceeded the depth limit of the ECT for rebar diameter estimation and it could only be used for detecting the presence of rebars and estimating cover depth. Images of the GPR results can be found in Appendix A, whereas more details can be found in deliverable D10.1.

In the Nordic pilot, the GPR scans showed that the wooden studs, the heating elements and some of the existing layers inside the walls and flooring (such as the insulation layer) could be identified. Areas of potential higher moisture or/and voids were also highlighted. Other features were also observed in the data that could correspond to meshing or cabling inside of the walls. Some of the scanning locations and images of the results are presented in Appendix B, whereas more information on the results can be found in deliverable D10.3.

## 4.5. Hardware

### 4.5.1. GP8800 sensor

The GP8800 GPR sensor was first manufactured by Proceq in 2017. It is a handheld SFCW GPR system ideal for small and congested areas. On top of the sensor, the removable battery pack is magnetically clamped. This pack also holds a USB-C charging port and a USB-C port for connecting the probe to the iPad with a cable if needed. Most of the time, however, the probe is operated wirelessly via Wi-Fi.

The sensor can be powered up by pressing one of the two buttons on either side. Once the button is pressed, a blue light on the top of the sensor will start flashing. When the light becomes stable, the probe is ready for use.

When the device is connected to the app and a new data collection is started, a measurement can be started/stopped by short-pressing one of the two buttons on either side. When collecting measurement

lines of specified length (such as in an area scan), the distance is measured by the encoder wheel and a sound will play when this length has been reached to let the user know that the line has been collected.

The encoder wheel can be unmounted and mounted to different sides but also rotated 90 degrees to allow scanning with different antenna orientation. The device is operated in direct contact with a surface to allow for the encoder wheel to spin as distance/movement is what triggers data collection.

#### 4.5.2. PM8000 sensor

The PM8000 sensor is an ECT system manufactured by Proceq. The sensor can be used on its own as standalone or attached to an encoder cart. If measurements are performed in standalone mode, the results are shown on the organic light-emitting diode (OLED) screen and no connection to the acquisition software is required. This is mainly used to perform simple spot measurements. When connected to the iPad PM app, the device can also be placed in the cart. The connection is established wirelessly via Bluetooth. This is used for scanning larger areas and to visualize the acquired data in different forms.

First, the batteries need to be inserted into the battery case integrated within the probe. Then, the probe can be powered up by the on/off button. If a cart is to be used, the cart should be attached first before switching on the device.

This sensor is unaffected by non-conductive materials but is highly affected by conductive materials at a close proximity to the sensor. Therefore, all metallic objects need to be removed before the measurements are initiated. Before start measuring, calibration is required for this sensor to correct any drifts due to temperature or other external effects. This is performed by holding the probe in free space with no metallic objects around. It is recommended to perform a calibration every 5 minutes.

Visual indicators in the form of arrows and centre line can be found on the probe which indicate the proximity of a metallic element. When the probe is directly above a metallic object such as a rebar in concrete, the centre line will light up. When the probe is in close proximity to, but not directly on top, a metallic object, the right or left arrow indicators will light up to show towards which direction, the metallic object can be found.

The probe has two modes, standard and deep. In standard mode, the rebar diameter can be estimated, and this mode can be used for scanning up to 63 mm depth. The deep mode can be used for up to 180 mm depth to detect the presence of rebars and concrete cover depth only but not for diameter estimation.

### 4.6. Software

#### 4.6.1. GP app

The GP app is the application that controls the GPR GP8800 probe. This app can be downloaded and installed only on an iPad via the App Store. In order to use the functionalities provided by the GP app, a subscription license is required, and the operator needs to sign in to the app with their account details. The main interface of the GP app with the menus for signing in, connecting to the probe and the data menu can be seen in Figure 11. From the Data menu, a new measurement can be started but also previously collected measurements can be visualized.

Connection to the probe can be made by navigating to the Probe menu in the main screen of the GP app and scanning the unique probe QR code, which can be found on the probe's top surface after removing the battery pack. To connect, the probe must be fully powered on, and the iPad needs to have Wi-Fi connectivity enabled. Alternatively, the probe can be connected to the iPad using a USB-C cable where in this case the serial number of the probe is detected automatically.

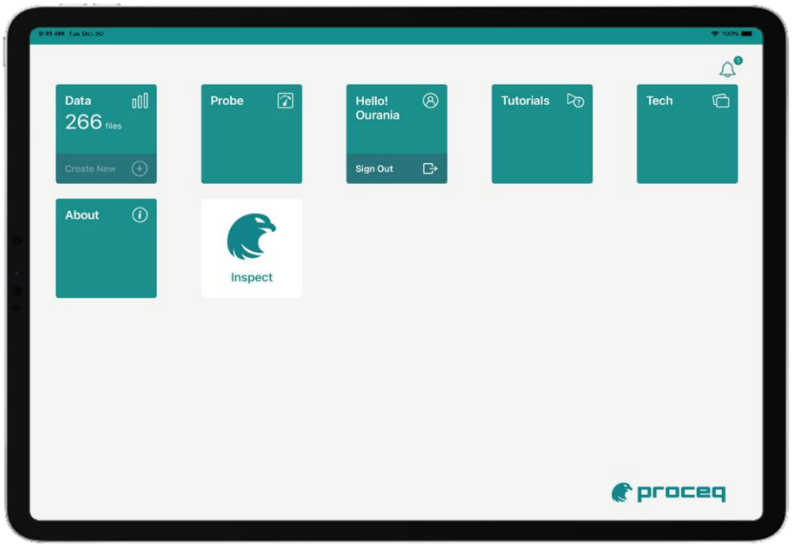


**Figure 11. The main interface of the GP app with the menus for signing in, connecting to the probe, the data menu and tutorials.**

After connecting, a new measurement can be created. Before start measuring, certain settings need to be set in the app:

- Measuring mode (set to Area scan in this case) and Repetition rate (scans/cm) which are both in the Measuring Presets menu
- Area scan dimensions and spacing which are set by editing the displayed grid

Figure 12 shows the interface for creating a new area scan measurement. The measuring presets options that need to be set are highlighted with a box, whereas the options for selecting the size of the area scan and spacing between the lines are marked with circles.

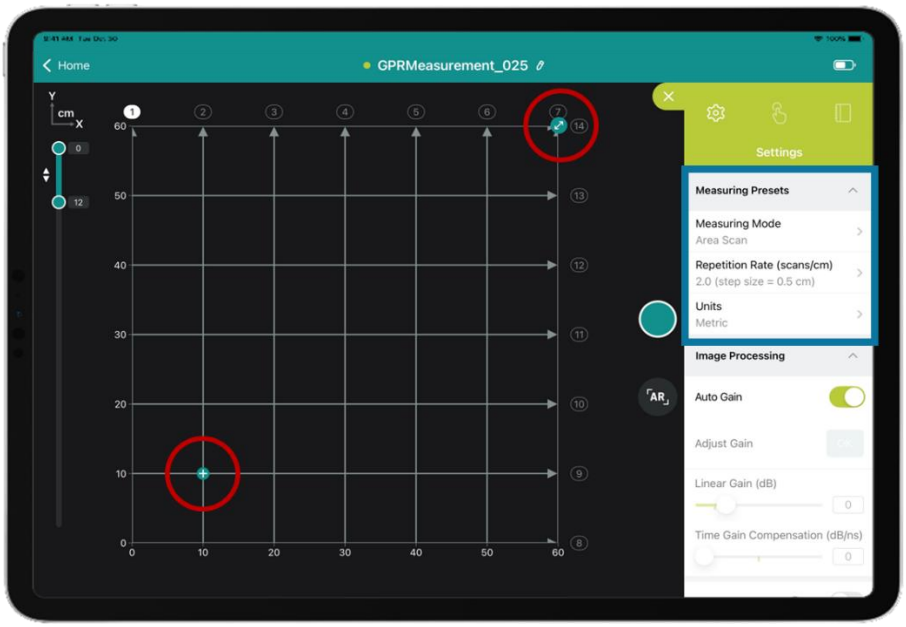


**Figure 12. Parameters need to be set in the app before starting an area scan. The box highlights the measuring presets to be chosen, whereas the circles show the buttons for selecting area scan size and spacing.**

After collection, the data can be visualized in review mode. Also, some basic processing can be performed in the GP app such as auto gain and dielectric calibration. This processing can be done both live during data collection, or after in review mode. A logbook is also recorded with the data collection information and any changes made.

Both the B-scans and the slices are available during and after data collection. With two finger swipes top-down, the different views can be displayed in addition to isosurfaces in 3D. The GP app also includes an augmented reality (AR) view of the depth slice and the isosurface views. For this to work, the provided grid paper is needed that includes the Proceq marker. This is necessary as this marker is the reference point for where the data should be projected onto the iPad. An example of an exported snapshot using the AR feature is given in Figure 13. This example is from the Nordic case study and the hidden vertical wooden stud can be seen directly at the location of scanning.

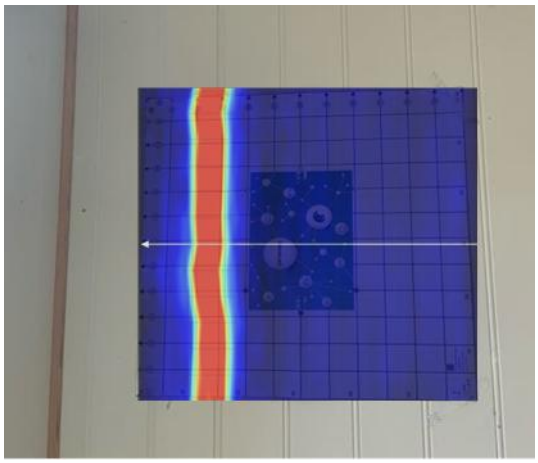

**Figure 13. Example of snapshot exported using the AR feature which projects the slice data on the iPad on top of the structure.**

Points of interest can be marked with tags by touch and hold. Different colours and icons can be used to distinguish between the different objects detected such as rebars, post-tension cables and backwall. Pictures of the site, text and voice notes can be made and attached to the measurement logbook through the app. The data can afterwards be exported in different file formats such as SEGY, which is a standard geophysical format, as snapshots or export HTML and DOCX reports.

### 4.6.2. PM app

The PM app is the application that controls the ECT PM8000 probe. This app can be downloaded and installed only on an iPad via the App Store. Similarly to the GP app, to use the functionalities provided by the PM app, a subscription license is required, and the operator needs to sign in to the app with their account details. A single account can be used to sign in to both the GP and PM app and all the measurements from each probe will be stored under this account; however, a different subscription is required for each sensor. An image of the main screen of the PM app can be seen in Figure 14.

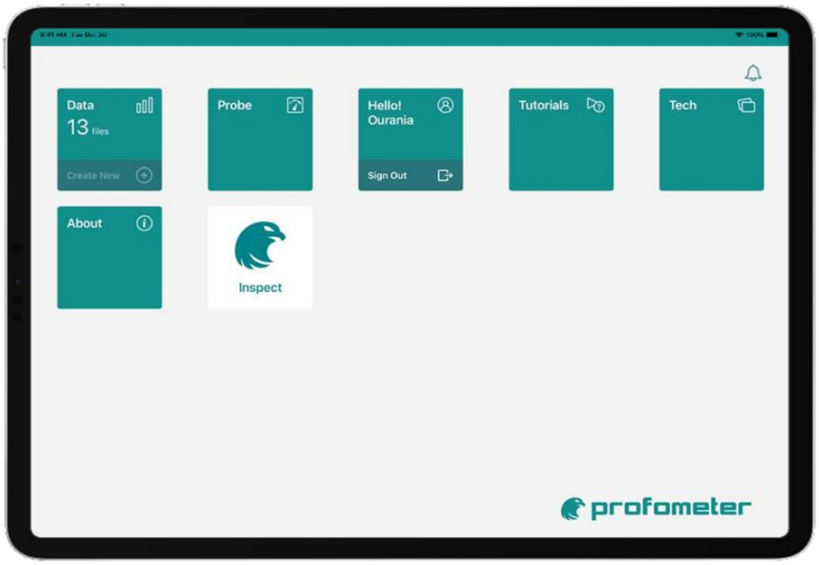


**Figure 14. Main interface o the PM app from which the probe connectivity, measurement menu and tutorials can be found.**

Once the probe is on, it can be connected to the app by going to the Probe menu via Bluetooth and thus Bluetooth must be enabled on the iPad. Once connected, a new measurement can be initiated, and its parameters can be set. Similarly, an area scan mode is chosen for which we need to set the dimensions and spacings in the displayed grid. In addition, based on the rebar depth, the standard or deep mode is selected. The interface for selecting those options looks similar to the one for the GP app shown in Figure 12.

Different data views can also be seen in the PM app which include individual line scan view, area scan and some rebar statistics. Swiping top-down with two fingers allows for navigating between the views. The line scan view displays the signal strength from each rebar, the rebar diameter (if it is possible to measure) and concrete cover. Figure 15 illustrates an example of a PM8000 line scan with all the above parameters shown for each detected rebar. An example of an area scan which also shows the rebars detected in both the x and y directions can be seen in Figure 16. The PM app also offers a feature of aligning the rebars in case these are not well-aligned due to positioning or other issues.

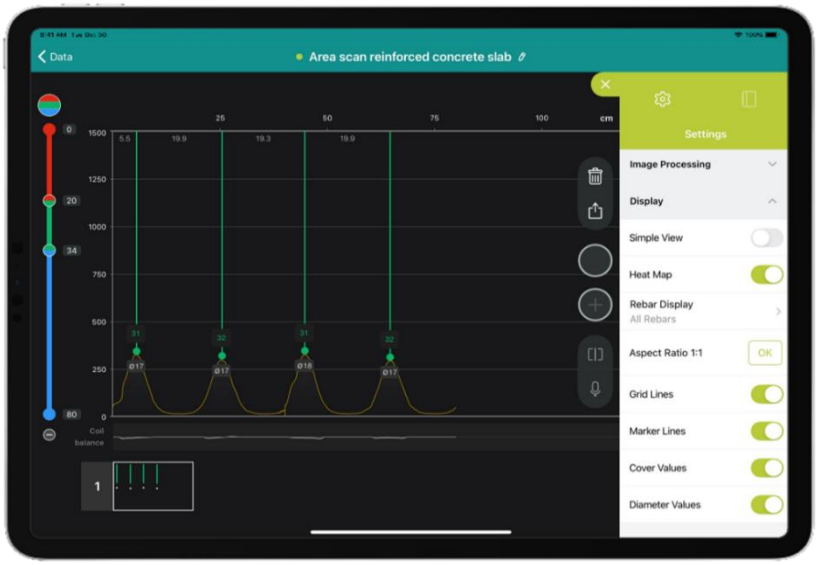


**Figure 15. Example of a PM8000 line scan view which shows the signal strength for each rebar, the rebar diameter and concrete cover depth values.**

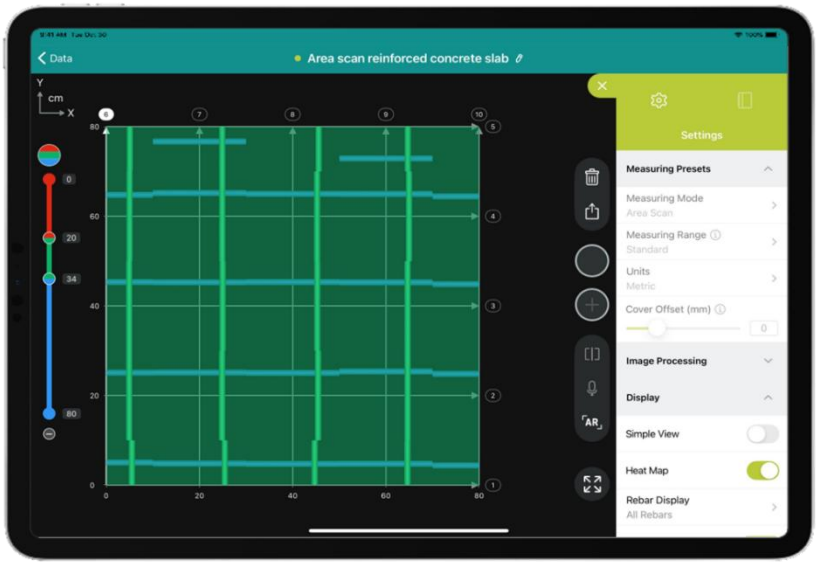


**Figure 16. Area scan with the PM8000 as shown in the PM app with the rebars at both directions being visible.**

The PM app also allows for the generation of heat maps which display the cover depth distribution across the scanning area and also allows for projecting this directly onto the structure via the AR feature

in the iPad. Similarly to the GP app, the data and measured values can be exported as HTML, DOCX or CSV files with snapshots or even a DXF file.

# 5. Challenges and limitations

This chapter will describe some of the challenges and limitations of the GPR and the ECT technology in general but also the limitations of the methodology proposed here.

## 5.1. Technical constraints of the technology

Despite its many advantages, similarly to other scanning techniques, GPR has also its limitations that can impact its effectiveness in certain scenarios.

One of the primary challenges is its penetration depth. GPR performance is significantly influenced by the conductivity of the medium. In materials such as clay-rich or wet soils, the radar signals tend to attenuate quickly, limiting how deep the radar can penetrate. This makes GPR less effective for surveys in areas with high conductivity as it causes signal loss, reducing the ability to detect deeper objects or structures and thus even large targets in areas with poor penetration conditions may go undetected.

In addition to the material influence on penetration, another limitation is the inherent trade-off between resolution and depth of a GPR system itself. GPR sensors operate across a range of frequencies, with lower frequencies providing greater penetration at the cost of reduced resolution, while higher frequencies offer finer resolution but are limited to shallow depths. This can make it challenging to balance the need for high-resolution imaging with the ability to penetrate deep into the ground, especially when both are needed in the same survey.

Thus, small features, such as rebars or wires, at shallow depths can be detected by a high-frequency antenna with high-resolution but might go undetected by a low-frequency antenna at the same of higher depths. Deep targets, such as large buried pipes, will be detected by a low-frequency antenna but might be missed by a high-frequency system due to penetration limitations. However, all systems (even high-frequency) have a limit in resolution and depth and if a target exceeds the system's capabilities, it will remain undetected. Depending on the type of survey, dual-frequency systems can be used that include a high-frequency and a low-frequency antenna to maximize the information received.

GPR performance can also be heavily influenced by surface conditions. The quality of data acquired can be significantly impacted by the roughness or nature of the scanning surface, as occurred in the Nordic pilot due to cladding. Uneven terrain or other surface obstructions can distort the radar signals and lead to poor-quality data. Additionally, the type of material on the surface, such as asphalt or concrete, can alter the radar's reflection properties, which complicates the interpretation of the results.

In urban environments, electromagnetic interference from electrical systems and metallic infrastructure can introduce external noise in the data, further degrading the signal quality and making the data interpretation harder.

One of the major limitations of GPR is the complexity of data interpretation. The radar signals collected by GPR are often difficult to interpret, as they can include multiple responses from different features and signal interference. This complexity requires significant expertise to accurately identify features and avoid misinterpretation of data. The need for trained professionals to analyze the data means that GPR is not as straightforward as other testing methods, and improper analysis can lead to incorrect conclusions. This makes the technology more challenging to use in situations where quick and straightforward data interpretation is required. In addition to experienced GPR users, a priori information on the survey area and the targets being sought is needed as the same GPR radargram can correspond to different scenarios.

While modern GPR systems have become more portable and advanced, cost and accessibility remain challenges. High-end systems, especially those with features like multichannel capabilities, can be expensive to acquire and maintain. Additionally, the need for specialized training to operate these systems effectively adds another layer of cost and complexity for potential users. In certain cases, field systems may still be bulky or require additional equipment, such as GPS for georeferencing, which can make large-scale surveys more logistically difficult and expensive.

Finally, the data processing involved in GPR surveys can be time-consuming. Although basic processing can be done on-site with the acquisition software, more advanced post-processing and visualization requires dedicated software. For large surveys, this can lead to a significant amount of data, requiring advanced computational power, time and expertise to analyze. The post-processing phase, while crucial for extracting accurate results, can be a bottleneck in the workflow, especially in projects with large datasets and hard deadlines.

Regarding the ECT sensor, one of its limitations is its penetration depth as it can be used accurately for estimating the rebar diameter only if the rebars are placed within the first 63 mm, after which the accuracy is reduced. For larger rebar depths > 63 mm, it is used for detecting the presence of rebars only and cover depth estimation. The cover depth accuracy is also reduced with depth.

Another challenge with the ECT sensor is conductive objects that might be placed nearby to the scanning location above ground within a ~400 mm sphere. These should be removed but if not possible, they can interfere with the useful signals from the rebars and influence the interpretation and conclusions. An additional limitation of this technology is the requirement for metallic objects, most commonly metallic reinforcement to be present in the structure for it to work and therefore, it cannot be used for structures where no reinforcement is present.

In conclusion, while GPR+ECT technology is a highly valuable and versatile tool, it has limitations and requires careful survey planning for each application and careful data interpretation. Both techniques are quite often used in conjunction and also combined with other techniques to provide a more comprehensive understanding of the subsurface.

## 5.2. Technical constraints of the proposed methodology

In addition to limitations of the technologies used, the suggested methodology in Task 2.5 has also its own limitations.

Although high-resolution is provided and the data collection is fast, both sensors used here are of small size and scanning larger areas such as a full building structure would require significantly more time. In the case of larger areas, poles could be attached to the probe for scanning the lines instead of handheld or utilize multichannel systems which have a wider scanning width and thus allow for scanning large areas faster.

Although in both pilot sites, the same data processing workflow worked well, for different and more complex case studies, a different processing sequence might be required. In addition, processing larger datasets on the iPad on-site is not efficient and dedicated post-processing software may therefore be required.

# 6. Conclusion

Deliverable D2.5 demonstrated the feasibility, methodology and efficiency of GPR+ECT technology in detecting and characterizing reusable construction materials which can be used in conjunction with a set of other methods for assessing building materials in support of circular construction practices. Both technologies enable the detection and characterization of hidden structural elements in a fast non-destructive manner, making them well-suited for selective deconstruction.

The focus of this deliverable was to provide a methodological framework starting from planning and data acquisition to processing and interpretation for scanning different types of construction structures with GPR + ECT technology and specifically for the purposes of the SUM4Re project. This framework was tested with two case studies. A timber residential building in Svalbard, Norway and a reinforced concrete application in an abandoned factory in San Sebastian, Spain.

Apart from the Spanish pilot which is common application of reinforced concrete to which GPR is applied, one achievement of this study was the application of GPR to a timber-based structure with multiple layers and hidden features and acquiring understanding of what information can be extracted from this type of structures with GPR. The pilot studies carried out in Spain and in Svalbard, in two highly different structures confirmed the adaptability of GPR across different construction types and environments.

Apart from the effectiveness of this approach, this document also highlights certain limitations and challenges. Some of the challenges are related to the surrounding material which influences that propagation and thus, the GPR data, the surface conditions which can also introduce affect the data and the complexity in data interpretation. Although the ECT results in the Spanish pilot were not favourable due to the high depth of the rebars which exceeded the depth limit of the sensor for diameter estimation, there are still many scenarios with shallow rebars in reinforced concrete slab that ECT can be highly effective and provide insights.

## ACKNOWLEDGEMENTS

We would like to thank all the partners from STORE NORSKE, SINTEF and MOYUA for their support during data collection. This project has received funding from the European Union's Horizon Europe research and innovation programme under grant agreement No. 101129961. Views and opinions expressed are those of the authors only and do not necessarily reflect those of the European Union or the European Health and Digital Executive Agency (HADEA). Neither the European Union nor the granting authority can be held responsible for them.

# BIBLIOGRAPHY

Daniels, D. J. *Ground penetrating radar, 2nd edition*. The Institution of Engineering and Technology, 2004.

Elseicy, A., M Solla and A. and Novo. “Preliminary Study on Automating Rebar Detection in Reinforced Concrete Structures Using YOLOv11 and GPR Data.” *13th International Workshop on Advanced Ground Penetrating Radar (IWAGPR)*. Thessaloniki, Greece, 2025.

Faris et al., N. “Automated rebar recognition and corrosion assessment of concrete bridge decks using ground penetrating radar.” *Automation in Construction* (2024).

Goodman, D. and S. Piro. *Multi-channel GPR in: GPR Remote Sensing in Archaeology. Geotechnologies and the Environment*. Berlin: Springer, 2013.

Patsia, O., A. Giannopoulos and I. & Giannakis. “Background Removal, Velocity Estimation, and Reverse-Time Migration: A Complete GPR Processing Pipeline Based on Machine Learning.” *IEEE Transactions on Geoscience and Remote Sensing* 61 (2023): 1-11.

Solla, M., et al. “Rebar detection: Comparison of stepped frequency continuous wave and pulsed GPR.” *Procedia Structural Integrity* 64 (2024): 293-300.

Wai-Lok Lai, W., X. and Dérobert and P. Annan. “A review of Ground Penetrating Radar application in civil engineering: A 30-year journey from Locating and Testing to Imaging and Diagnosis.” *NDT & E International* (2018): 58-78.

Warren, C., A. Giannopoulos and I. & Giannakis. “gprMax: Open source software to simulate electromagnetic wave propagation for Ground Penetrating Radar.” *Computer Physics Communications* (2016): 163-170.

# SUM4Re

Creating materials banks
from digital urban mining

# APPENDICES

Funded by the European Union. Views and opinions expressed are however those of the author(s) only and do not necessarily reflect those of the European Union. Neither the European Union nor the granting authority can be held responsible for them.

Funded by
the European Union

# LIST OF APPENDICES

APPENDIX A RESULTS FROM THE NORDIC PILOT ..... 41
APPENDIX B RESULTS FROM SPANISH PILOT IN JOLASTOKIETA ..... 45

# LIST OF FIGURES IN THE APPENDICES

Figure 1-A. Photos from the GPR data collection from internal scans (top) and external scans (bottom). ..... 41
Figure 2-A. Depth slice from scan location VIII, where the heating elements can be observed. ..... 41
Figure 3-A. a) Depth slice at location XV that shows the underfloor heating and b) B-scan sample from floor scan XII in the second floor apartment. ..... 42
Figure 4-A. a) Depth slice at wall location XIII showing the vertical wooden stud identified, b) Line 7 B-scan at location XIII with the different layer interfaces and the wooden stud response seen, c) Location of line 22 in position XIII and d) Line 22 B-scan with a series of hyperbolas at the same depth corresponding possibly to some kind of meshing or cabling. ..... 42
Figure 5-A. Results from area scan on internal wall between living room and bedroom of second floor apartment. ..... 43
Figure 6-A. Internal scans on bathroom wall between the two apartments of the second floor. ..... 43
Figure 7-A. a) Y-directed B-scan at external position J1 illustrating the clutter caused by the cladding and b) X-directed scan at external position G showing other responses observed. ..... 44
Figure 8-A. External wall scan position K and B-scan examples showing the variations observed in the GPR data in this wall area. ..... 44
Figure 1-B. a) First area scan location, b) GPR B-scan showing the reinforcement, c) GPR slice at ~12 cm depth, d) Reinforcement as isosurfaces in 3D, e) GPR slice at ~17 cm depth and f) Line 4 B-scan. ..... 45
Figure 2-B. a) and b) Second area scan location, c) and d) Y-directed GPR B-scans, e) and f) X-directed GPR B-scans ..... 46
Figure 3-B. a) Third area scan location, b) GPR line 21, c) GPR slice at ~16 cm depth which also illustrated the position of line 21 with a dashed line, d) Isosurfaces of reinforcing mesh, e) and f) Detected element at ~24 cm depth. ..... 47
Figure 4-B. Target at ~30 cm depth in third area as shown in a) GPR depth slice and b) GPR B-scan line 8. Line 8 is also illustrated with a dashed line on the slice in a). ..... 48
Figure 5-B. Third area: a) Line 2 B-scan and b) Line 23 B-scan with the clutter region highlighted at the top which indicates possible moisture and/or voids. ..... 48
Figure 6-B. a) Fourth area scan location, b) GPR slice at ~5 cm depth, which also illustrates the position of line 23 with a dashed line, c) GPR line 23, d) GPR Slice at ~19 cm depth and e) Isosurfaces of reinforcing mesh. ..... 49
Figure 7-B. Unidentified response around 13 cm depth as seen in a) GPR slice and b) GPR B-scan line 19 where it is marked with an ellipse. ..... 49
Figure 8-B. a) Flat response around 6 cm depth and b) Amplitude map of the response showing weaker and stronger healthier regions. ..... 50

## APPENDIX A Results from the Nordic pilot

Some of the results in the form of annotated images from the Nordic pilot data are provided in this Appendix. More information on the results and data interpretation can be found in deliverable D10.3.

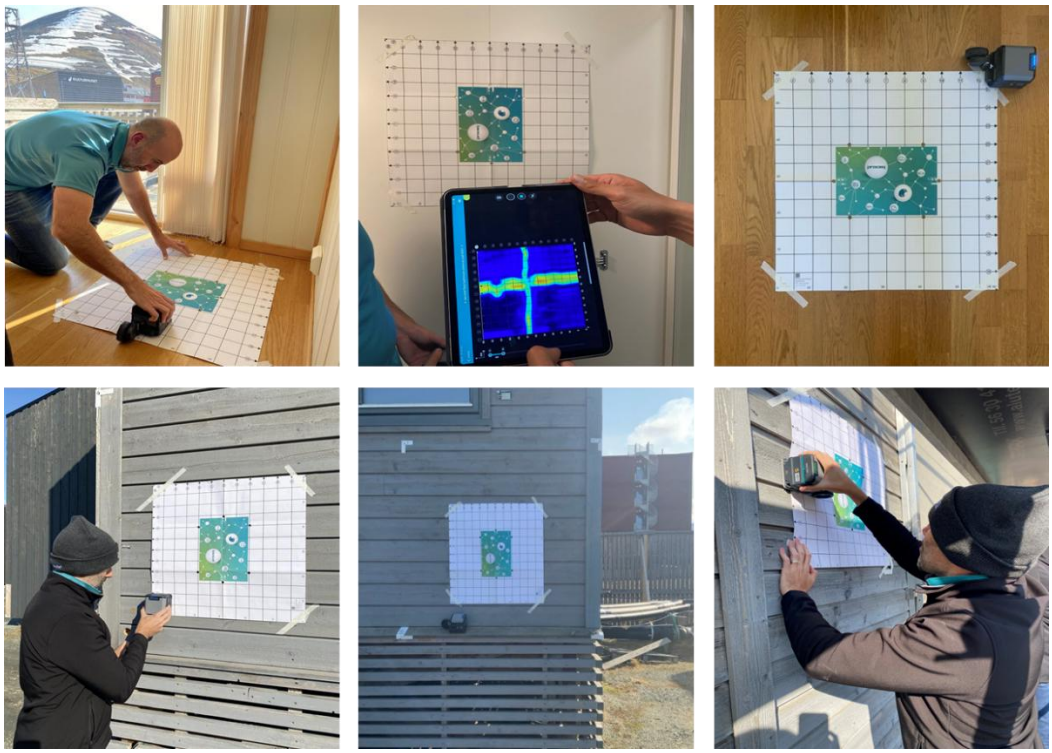

*Figure 1-A. Photos from the GPR data collection from internal scans (top) and external scans (bottom).*

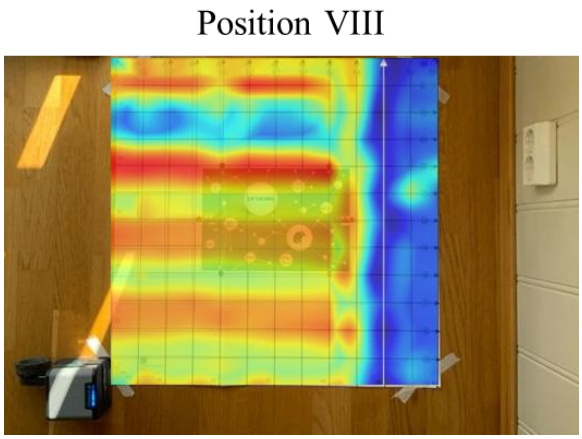


*Figure 2-A. Depth slice from scan location VIII, where the heating elements can be observed.*

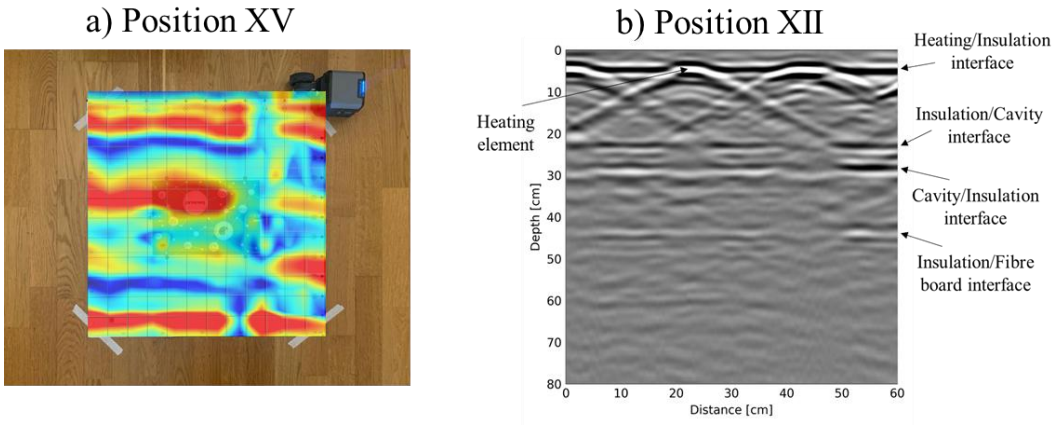


*Figure 3-A. a) Depth slice at location XV that shows the underfloor heating and b) B-scan sample from floor scan XII in the second floor apartment.*

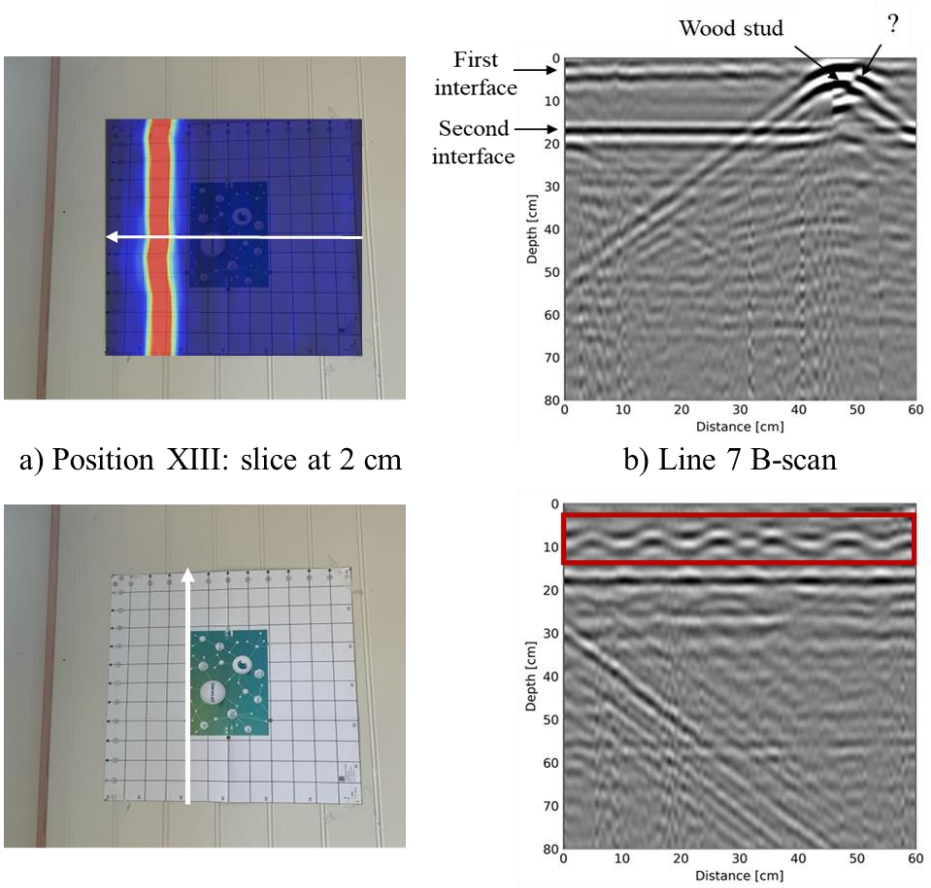


*Figure 4-A. a) Depth slice at wall location XIII showing the vertical wooden stud identified, b) Line 7 B-scan at location XIII with the different layer interfaces and the wooden stud response seen, c) Location of line 22 in position XIII and d) Line 22 B-scan with a series of hyperbolas at the same depth corresponding possibly to some kind of meshing or cabling.*

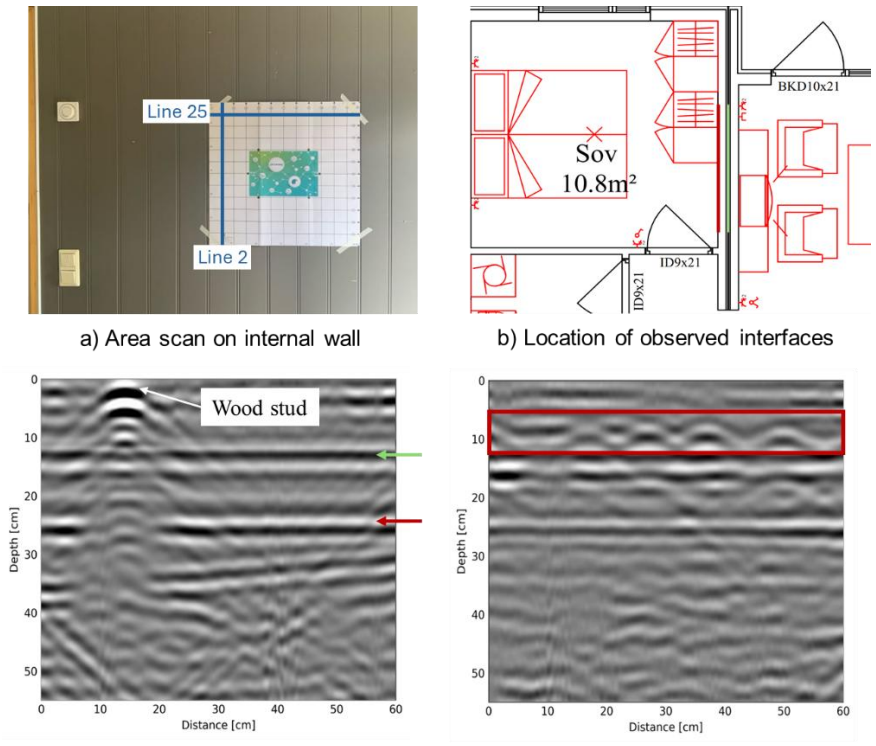


a) Area scan on internal wall

b) Location of observed interfaces

c) B-scan line 25

d) B-scan line 2

*Figure 5-A. Results from area scan on internal wall between living room and bedroom of second floor apartment.*

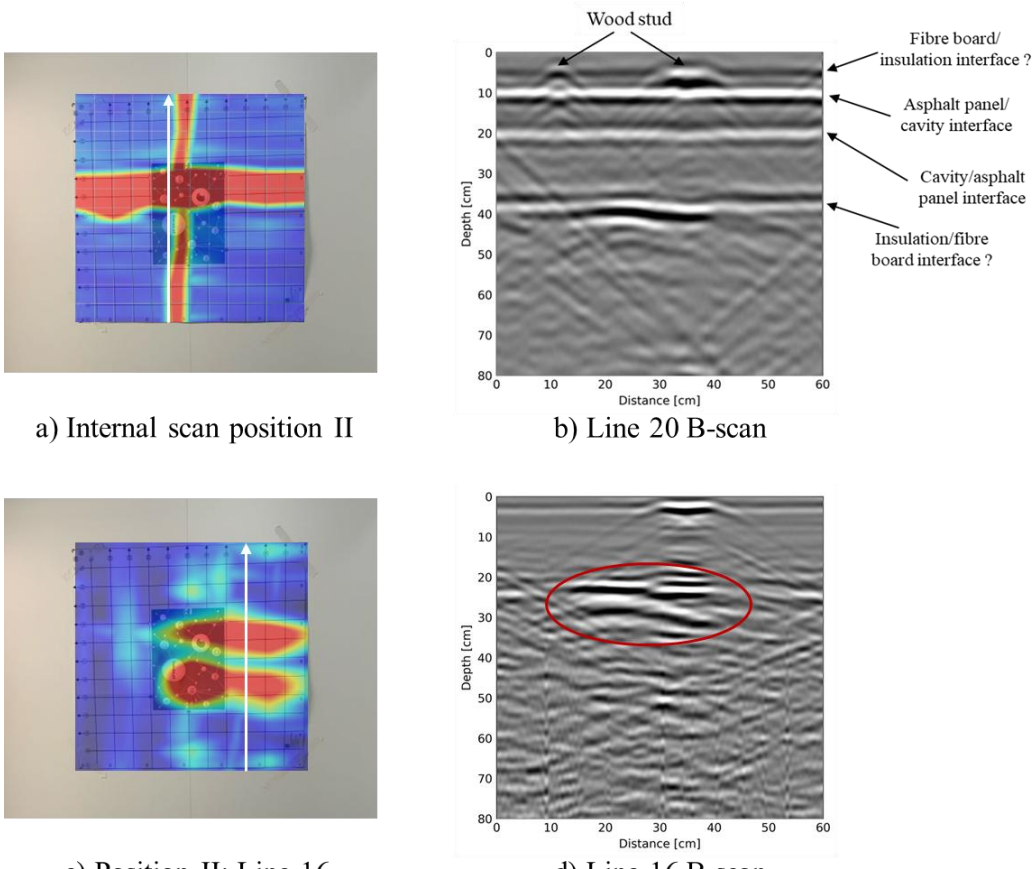


a) Internal scan position II

b) Line 20 B-scan

c) Position II: Line 16

d) Line 16 B-scan

*Figure 6-A. Internal scans on bathroom wall between the two apartments of the second floor.*

a) External position J1: y-directed scan

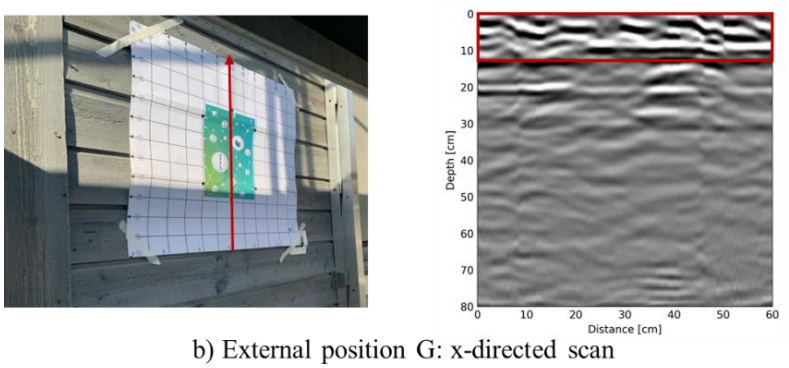


b) External position G: x-directed scan

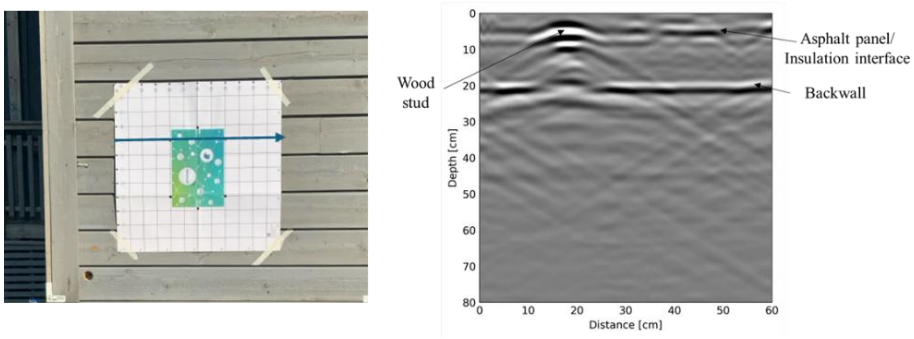


*Figure 7-A. a) Y-directed B-scan at external position J1 illustrating the clutter caused by the cladding and b) X-directed scan at external position G showing other responses observed.*

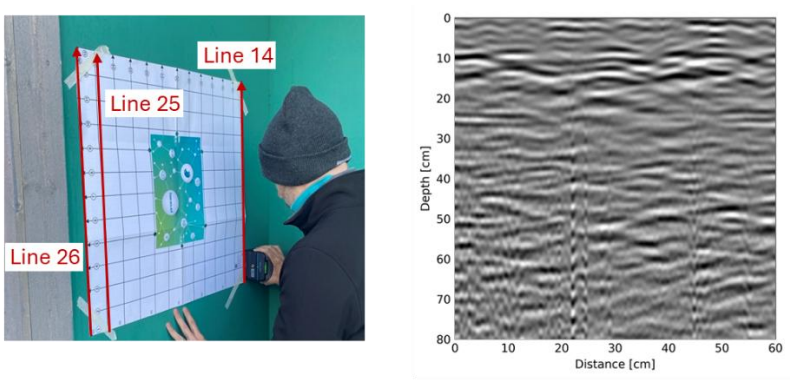


a) External scan position K

b) Line 14 B-scan

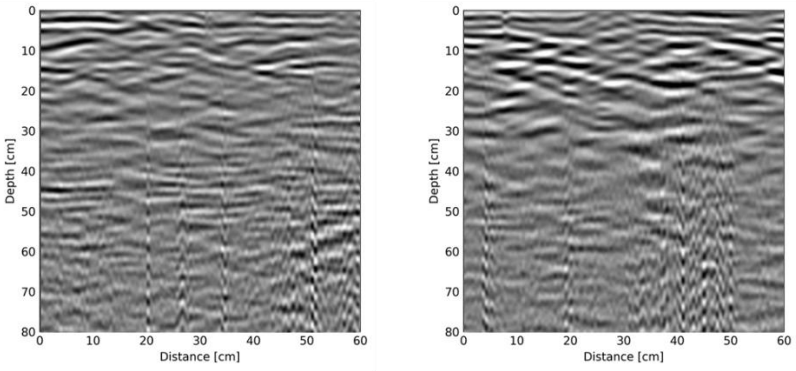


c) Line 25 B-scan

d) Line 26 B-scan

*Figure 8-A. External wall scan position K and B-scan examples showing the variations observed in the GPR data in this wall area.*

## APPENDIX B Results from Spanish pilot in Jolastokieta

Some of the results in the form of annotated images from the Spanish pilot data are provided in this Appendix. More information on the results and data interpretation can be found in deliverable D10.1.

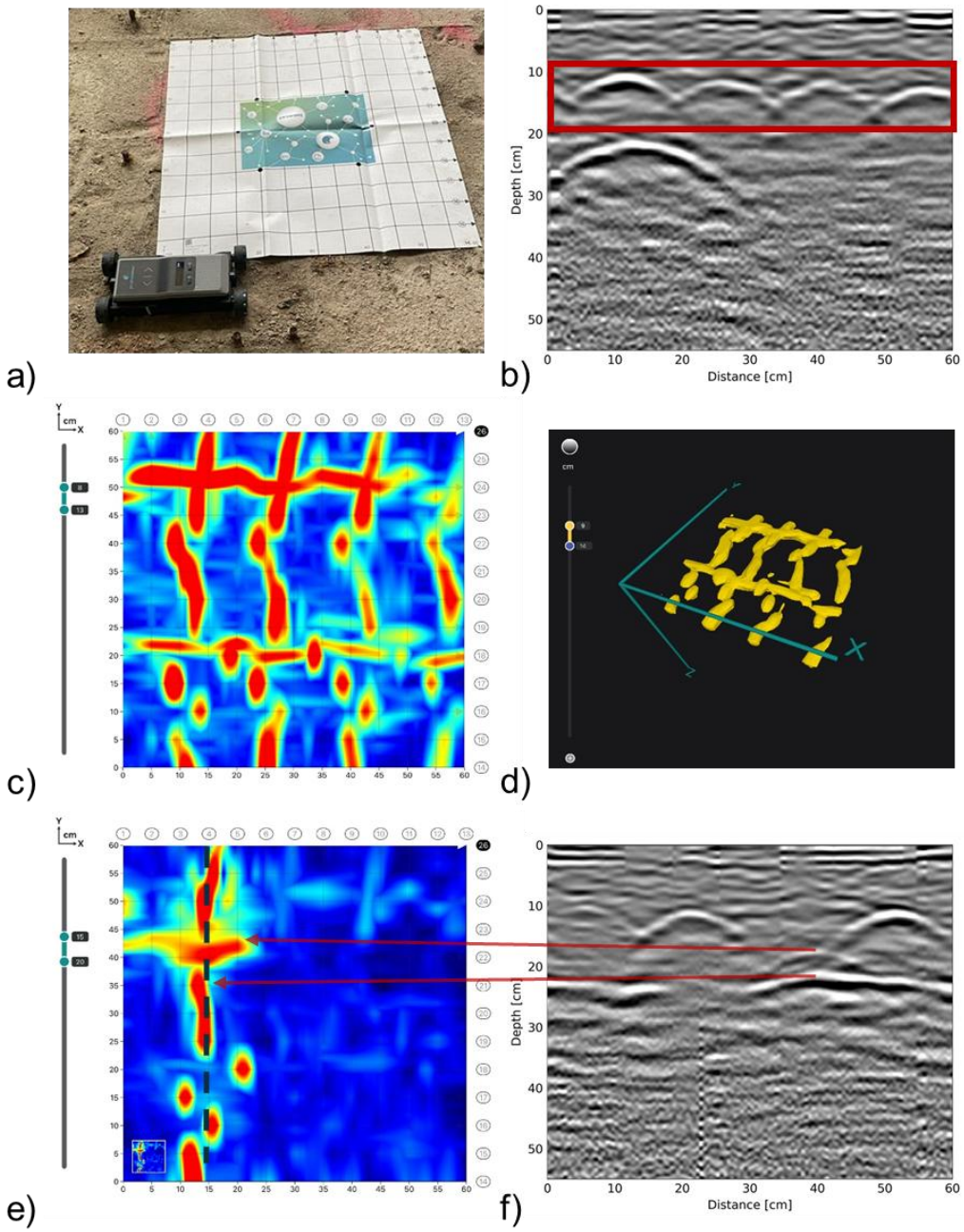


*Figure 1-B. a) First area scan location, b) GPR B-scan showing the reinforcement, c) GPR slice at ~12 cm depth, d) Reinforcement as isosurfaces in 3D, e) GPR slice at ~17 cm depth and f) Line 4 B-scan.*

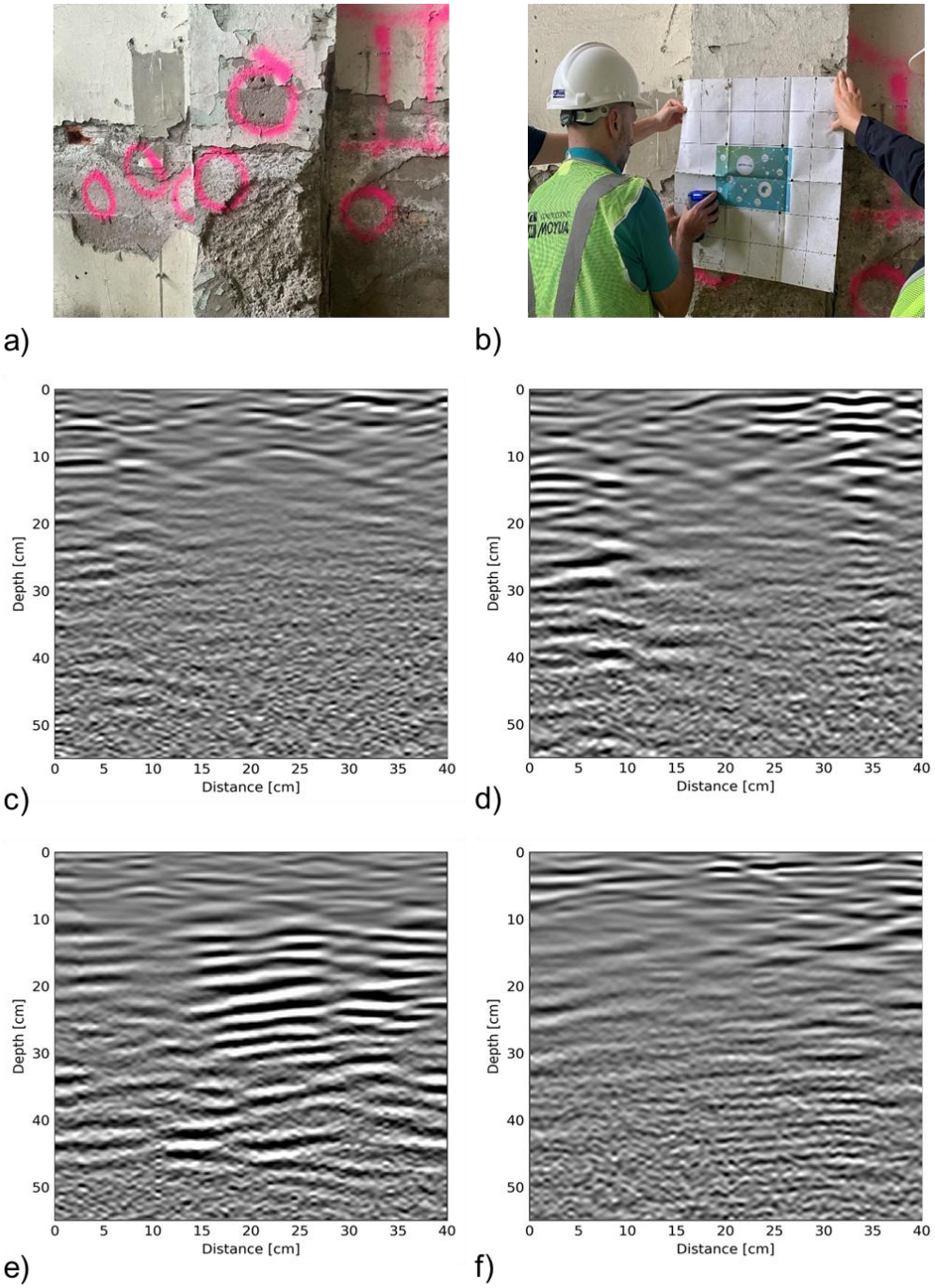


*Figure 2-B. a) and b) Second area scan location, c) and d) Y-directed GPR B-scans, e) and f) X-directed GPR B-scans.*

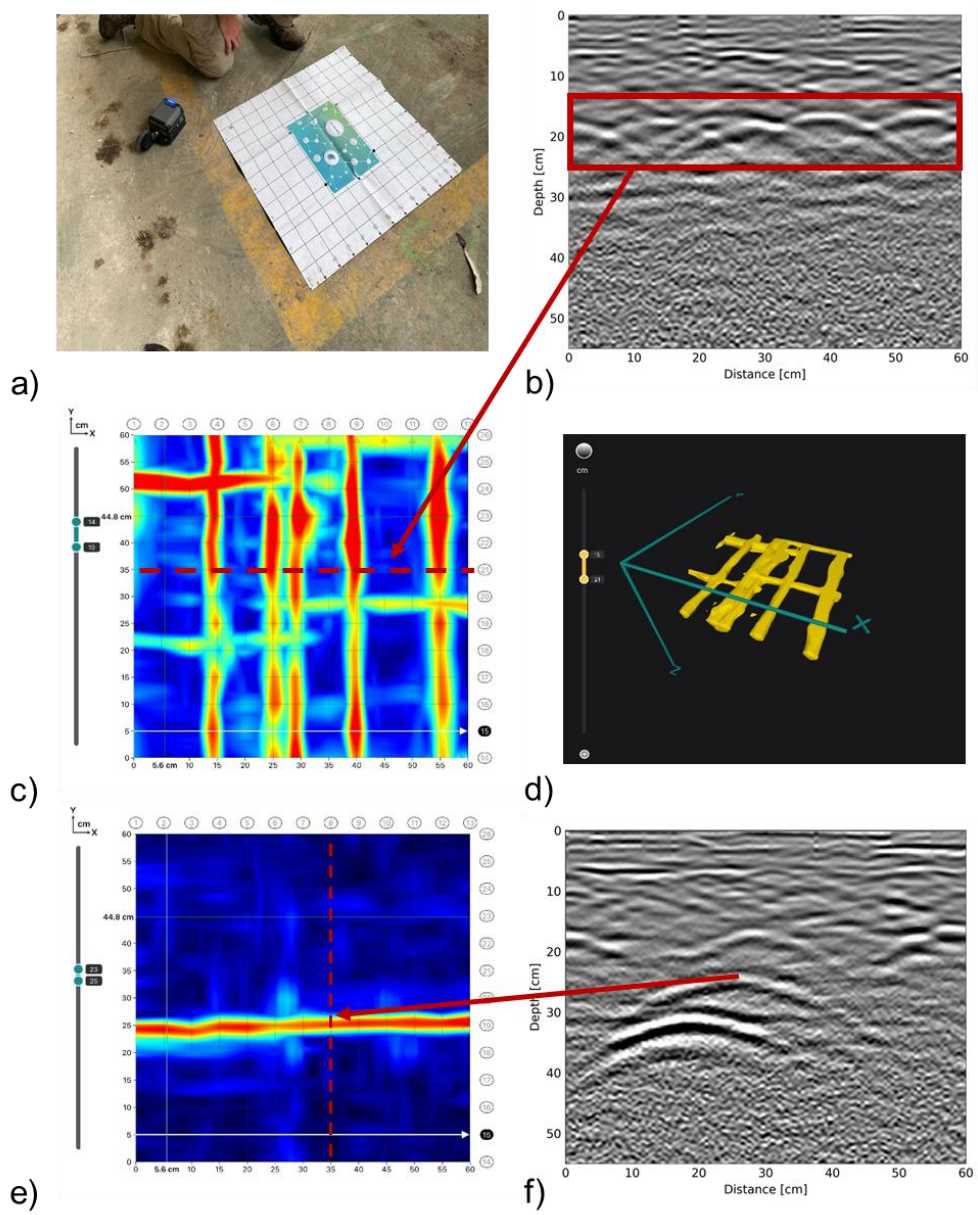


*Figure 3-B. a) Third area scan location, b) GPR line 21, c) GPR slice at ~16 cm depth which also illustrated the position of line 21 with a dashed line, d) Isosurfaces of reinforcing mesh, e) and f) Detected element at ~24 cm depth.*

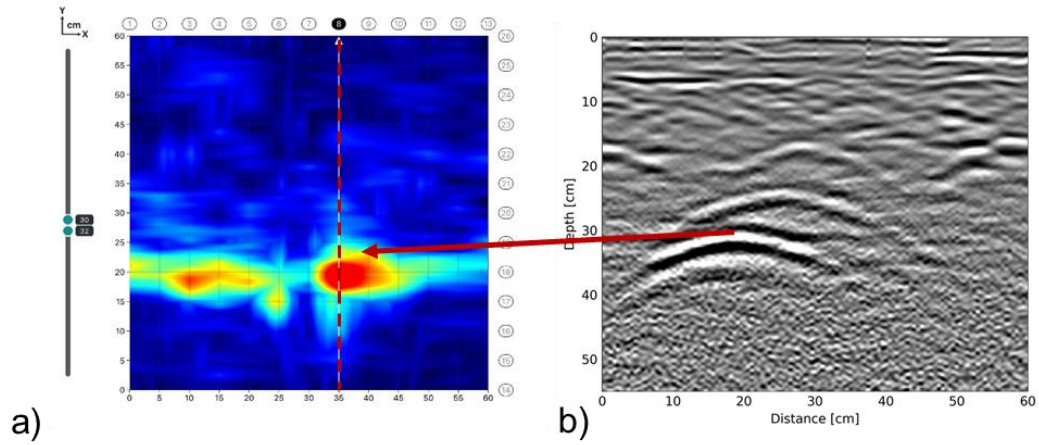


*Figure 4-B. Target at ~30 cm depth in third area as shown in a) GPR depth slice and b) GPR B-scan line 8. Line 8 is also illustrated with a dashed line on the slice in a).*

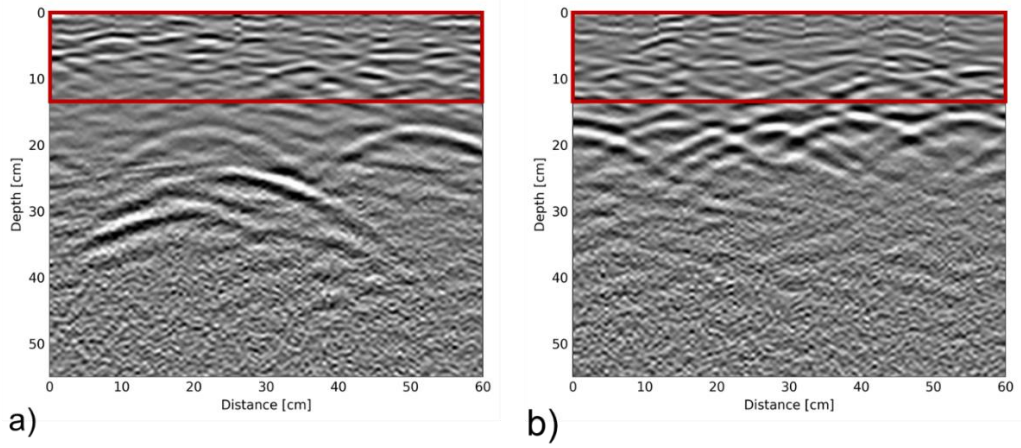


*Figure 5-B. Third area: a) Line 2 B-scan and b) Line 23 B-scan with the clutter region highlighted at the top which indicates possible moisture and/or voids.*

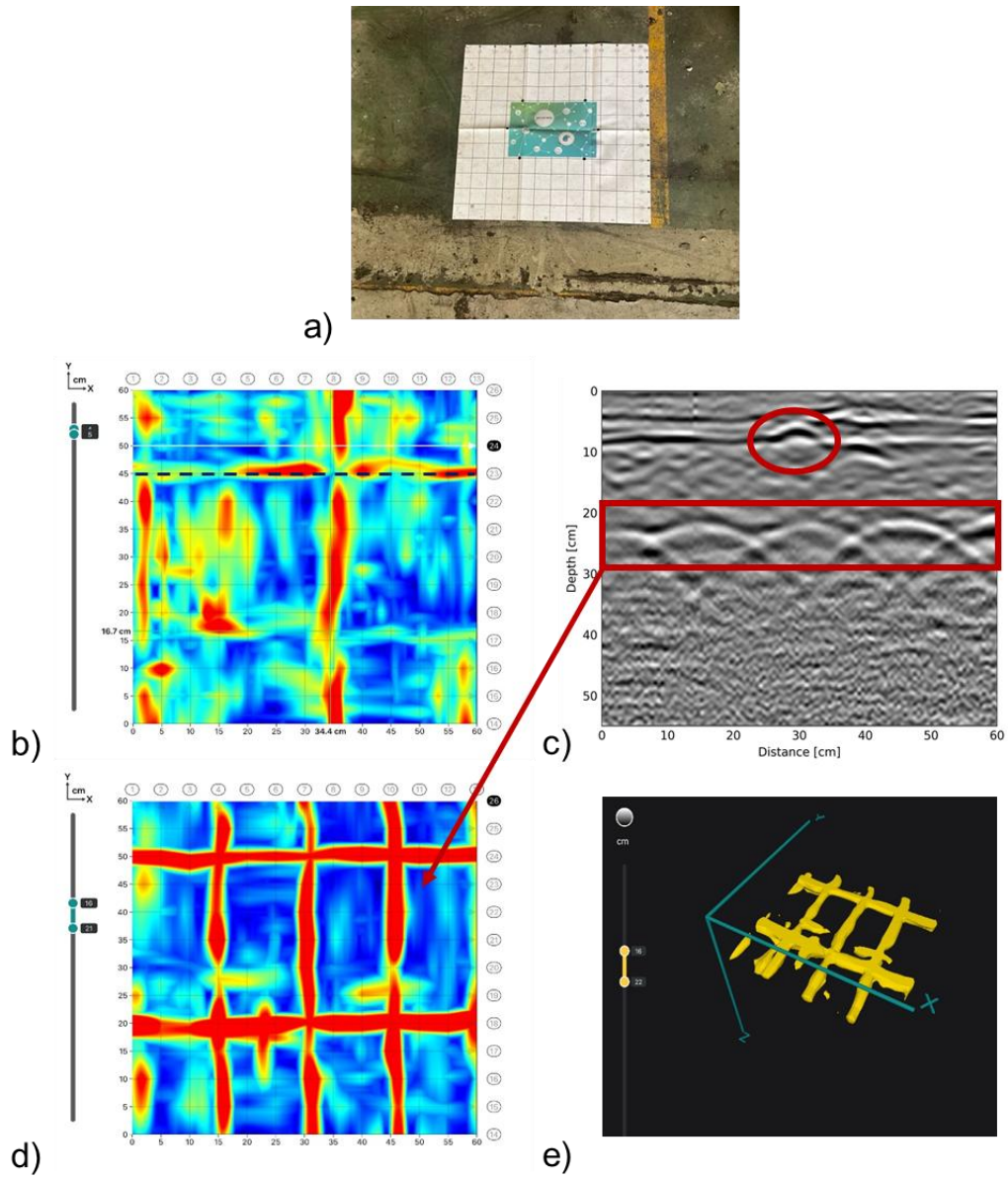


*Figure 6-B. a) Fourth area scan location, b) GPR slice at ~5 cm depth, which also illustrates the position of line 23 with a dashed line, c) GPR line 23, d) GPR Slice at ~19 cm depth and e) Isosurfaces of reinforcing mesh.*

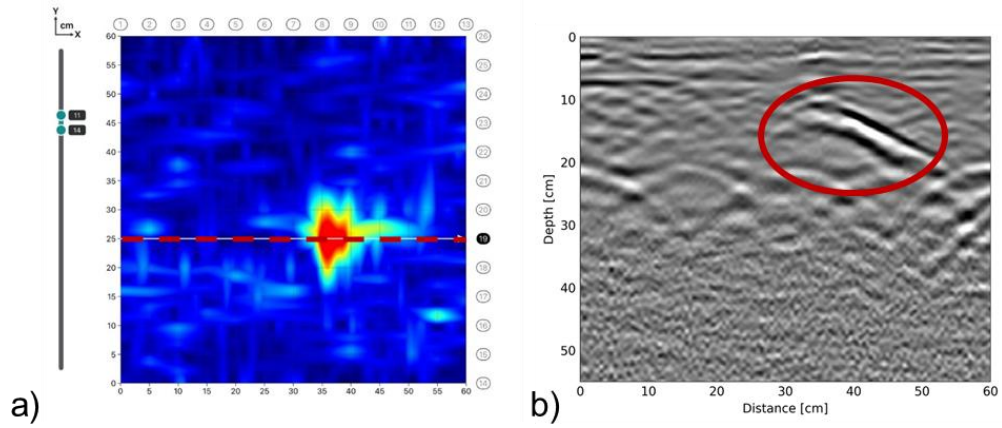


*Figure 7-B. Unidentified response around 13 cm depth as seen in a) GPR slice and b) GPR B-scan line 19 where it is marked with an ellipse.*

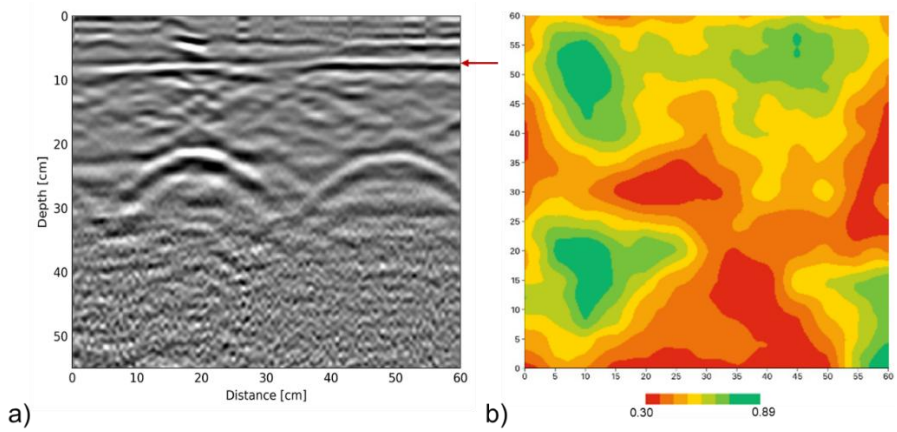


*Figure 8-B. a) Flat response around 6 cm depth and b) Amplitude map of the response showing weaker and stronger healthier regions.*

# SUM4Re

Creating materials banks
from digital urban mining

www.sum4re.eu sum4re@uvigo.gal SUM4Re SUM4Re_EU

Funded by the European Union. Views and opinions expressed are however those of the author(s) only and do not necessarily reflect those of the European Union. Neither the European Union nor the granting authority can be held responsible for them.

Funded by the European Union